Hindawi
Journal of Chemistry
Volume 2023, Article ID 8199000, 28 pages
https://doi.org/10.1155/2023/8199000

Research Article

Hydrogeochemical Characterization and Appraisal of Groundwater Quality in Yisr River Catchment, Blue Nile River Basin, Ethiopia, by Using the GIS, WQI, and Statistical Techniques

Abebaw Demelash,[1] Abunu Atlabachew,[2] Muralitharan Jothimani,[3] and Abel Abebe[3]

[1]*Department of Geology, Faculty of Natural and Computational Sciences, Woldia University, Woldia, Ethiopia*
[2]*Faculty of Water Resources and Irrigation Engineering, Arba Minch Water Technology Institute, Arba Minch University, Arba Minch, Ethiopia*
[3]*Department of Geology, College of Natural and Computational Sciences, Arba Minch University, Arba Minch, Ethiopia*

Correspondence should be addressed to Muralitharan Jothimani; muralitharan.jothimani@amu.edu.et

Received 25 January 2023; Revised 6 March 2023; Accepted 5 April 2023; Published 18 April 2023

Academic Editor: Shankar Karuppannan

Groundwater is a primary drinking, agricultural, domestic, and nondomestic water source in Ethiopia's Yisr River watershed of the Blue Nile River basin. There has been no systematic investigation of the hydrogeochemical properties of groundwater in the research area. The study investigated the hydrogeochemical parameters of groundwater in the catchment to find out if it is fit for drinking and irrigation. A total of 26 samples of groundwater were collected and analyzed for seventeen parameters, including pH, temperature, EC, TDS, TH, K^+, Na^+, Ca^{2+}, Mg^{2+}, Fe^{2+}, Cl^-, HCO_3^-, CO_3^{2-}, SO_4^{2-}, F^-, PO_4^{2-}, and NO_3^-. The data were processed and evaluated using integrated hydrogeochemical techniques, including individual ionic signatures, interionic ratios, and multivariate statistical methods, such as multiple correlation analysis, principal component analysis, and hierarchical cluster analysis. The water quality index (WQI) and Na%, PI, RSC, SAR, EC, TDS, and MH were used to judge the quality of water for drinking and irrigation, respectively. The box plot diagram shows the dominant ions in descending order of $Ca^{2+} > Mg^{2+} > Na^+ > K^+$ and $HCO_3^{2-} > Cl- > SO_4^{2-} > NO_3^- > F^-$ for cations and anions, respectively. The chemical composition of shallow wells and springs indicates freshwater. At the same time, the deep groundwater wells are brackish. The two-factor loadings (principal component analysis) were used to explain the existence of anthropogenic and geogenic sources. Three clusters are identified in the dendrogram. The third cluster has the most significant linkage distance among all the clusters. This means that the groundwater sample in this cluster is geochemically different from the other two clusters, and that this cluster is made up of only deep wells. Water quality indices showed that water quality ranged from excellent to very poor, with the majority (53.85%) being excellent and 26.9% being good. The results of the calculated indices for agricultural water quality indicated that the water quality in most collected samples was in the good and excellent categories; however, the EC, RSC, MH, and TDS indices in deep groundwater wells were found to be hazardous. The findings of this study are useful for understanding groundwater sustainability for various reasons. However, they are also helpful in supporting water management and protection in the future.

1. Introduction

The saturation zone of an aquifer contains groundwater at various depths. Many elements, ions, and compounds can dissolve in groundwater because the water and rocks react with each other. Many factors influence groundwater quality, including mineral composition, dissolution and precipitation of minerals, anthropogenic activities, and seawater intrusion [1–5]. Safe drinking water services in Ethiopia are among the lowest in Sub Saharan Africa [6]. In Ethiopia, it is common for water sources, such as springs, streams, rivers, and seasonal ponds, to be unprotected and contaminated. In northern Ethiopia, including the study area, domestic water usage depends on groundwater [7].

There are no perennial rivers in the study area, except for the Yisr River, and a few flash types of seasonal streams. For this reason, people in the study area acquire water from groundwater resources such as wells and springs for domestics, livestock, and irrigation purpose.

Despite the lack of alternative water sources, groundwater is used for multiple purposes, including sustaining life owing to urban expansion and agricultural activities in the catchment. However, there has not been a full study of the hydrogeochemical properties of watersheds to help manage and save water in the future. Groundwater quality has been analyzed using various traditional graphical and statistical tools [8–13]. Geostatistical modelling and multivariate statistics must be used to fully understand and characterize groundwater quality for effective management [14–19]. With the help of geographic information system (GIS) technology, it is now easier to view, evaluate, and report groundwater quality over large areas. This tool analyses and shows hydrologic/hydrogeological data across space and time. It also provides valuable information regarding spatiotemporal variations.

GIS technologies can be used to study groundwater quality, map differences in water quality across space, predict subsurface flow, and set up networks for monitoring groundwater [20–23]. The water quality index (WQI) provides comprehensive information on water quality to assess the suitability of water for different applications. The WQI can also determine drinking water quality in any area and provide general information [24, 25]. The Water Quality Index looks at and rates several factors that affect water quality [26, 27].

Thus, in the outlook of the above, the present study aimed to conduct and evaluate the attributes of groundwater chemistry in the Yisr River catchment, Blue Nile River basin, Ethiopia, using hydrochemical signatures together with a combination of multivariate statistical analysis and graphical representations. More specifically, this study aimed to (1) investigate the physicochemical characteristics of groundwater using significant chemical constituents (major cations and anions) and minor ions. (2) identify the evolution of groundwater and the mechanisms controlling its chemistry, and (3) assess groundwater potability and agricultural viability. A groundwater management framework may help water resource management and development by considering the unique hydrogeochemistry and quality of groundwater for irrigation and drinking in this study area.

2. Materials and Methods

2.1. Location of the Study Area. The study area, the Yisr River catchment (Figure 1), lies on the northwestern plateau of the country, in the center of the Abay (Blue Nile) river basin (the largest basin in Ethiopia), in the Amhara regional state, West Gojjam zone. The study area contains portions of Bure and Jabitehinan Woreda. Geographically, it is bounded by 37°00′00″ to 37°12′00″ ′E longitude and 10°25′30″ to 10°51′0″N latitude. It covers an area of 318 km^2. The study area is 148 km southwest of Bahir Dar, the capital city of Amhara regional state.

2.2. Physiography and Drainage. The study area, the center of the Abay Basin, belongs to the northwestern massifs of Ethiopia and lies in the rolling plains at the foot of the Choke Mountains (recharge zone of the Abay Basin). The approximate altitude of the study area ranges from 1526 m to 2476 m. It has a low-lying, slightly rugged topography (Figure 2). There are no perennial rivers in the study area that have a direct hydrogeological impact on local aquifer systems, except for the Yisr River. The drainage patterns of the perennial (Yisr River) and flashy-type seasonal streams in the area were primarily parallel to the subdendritic pattern (Figure 2).

2.3. Geology of the Study Area. The Yisr River catchment study area consists of tertiary lower (TV1) and middle (TV2) basalt to quaternary pyroclastic cones and recently reworked eluvial and alluvial deposit sediments (Figure 3). TV1 is generally dark grey and is exposed as a continuous sheet. Megascopically, it is dark grey to light brownish-grey and yellowish-brown, and after, it has been exposed to the elements, it typically takes on a purple or reddish-brown hue. TV2 is usually exposed as continuous, sheet-like, or small block and fragmental outcrops. Megascopically, the upper basalt is dark grey to greyish, and when weathered, it is yellowish-brown to reddish-white or purplish in colour. It is a pyroxene-plagioclase phyric basalt,, and plagioclase phyric basalt with occasional olivine-pyroxene-plagioclase phyric basalt pockets interlayered with pyroclastic tuff. The pyroclastic flows exposed bare rock. It lies on top of the quaternary soil cover and frequently has bushy vegetation. These quaternary rocks commonly outcrop as pyroclasts of scoriaceous basalt-forming cones, forming isolated hills of conical shape and are unevenly distributed and vascularly coarse-grained. The cones had moderate-to-steep slopes. The pyroclasts show various colours in outcrops, such as light grey, dark grey, and purple varieties.

2.4. Soil of the Study Area. A large area of land in the research area is covered by Quaternary alluvial soil, which consists mainly of red to reddish-brown silty or clay soil with remains of basalt rock. The maximal thickness of soil revealed by the drilling is between five and 10 meters. Red or reddish-brown elluvial soil may suggest its in situ formation from basaltic rocks underneath the surface [28]. Alluvial soil is a product of the deposition of soil transported by water and gravel and clay deposits by the stream from the hill to the lower ground. It is exposed mainly in the south and southwest of the study area along stream valleys and their vicinity and in marshy locations. Figure 3 shows the geology map of the study area.

2.5. LULC. Broadly, four land use/land cover classes were identified as follows: (I) intensively cultivated agricultural land covering gently sloping and flat areas of the catchment. It comprised 78.5% of the study area and was mostly made up of scattered bushes and settlements (rural villages). (II) Bushes, shrubs, and grassland cover approximately 12.5% of the catchment area. (III) 6% of the investigated area comprised dense settlements (bure towns). Forests are present in the remaining 4%.

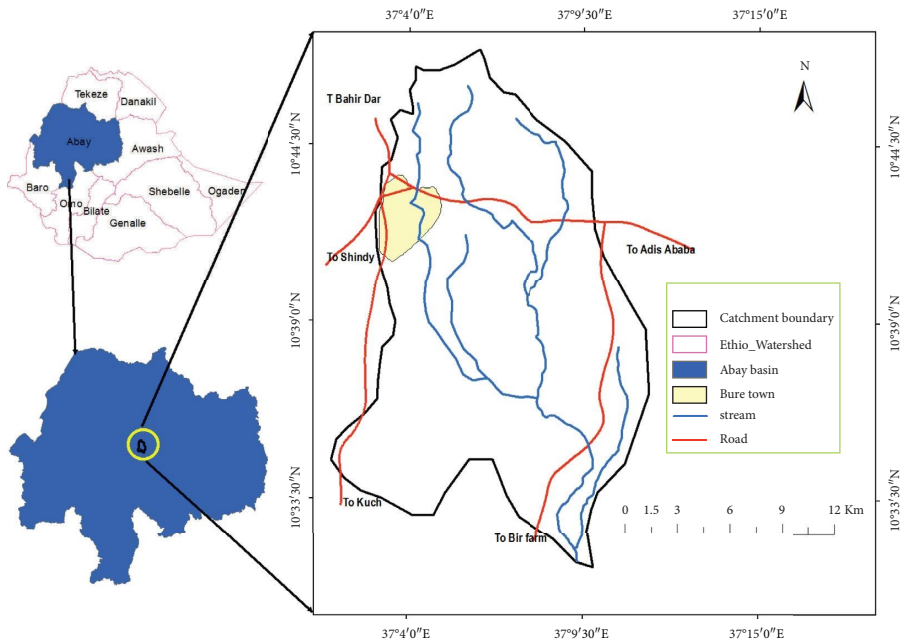

Figure 1: Location map and accessibility of the study area.

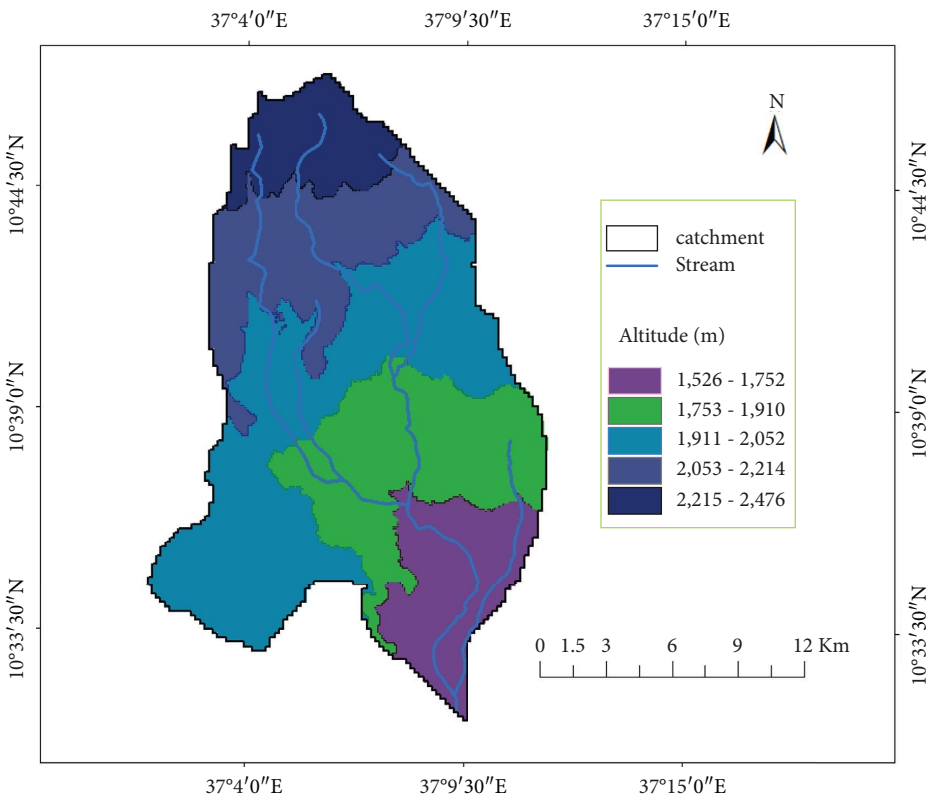

Figure 2: Drainage and elevation map of the catchment.

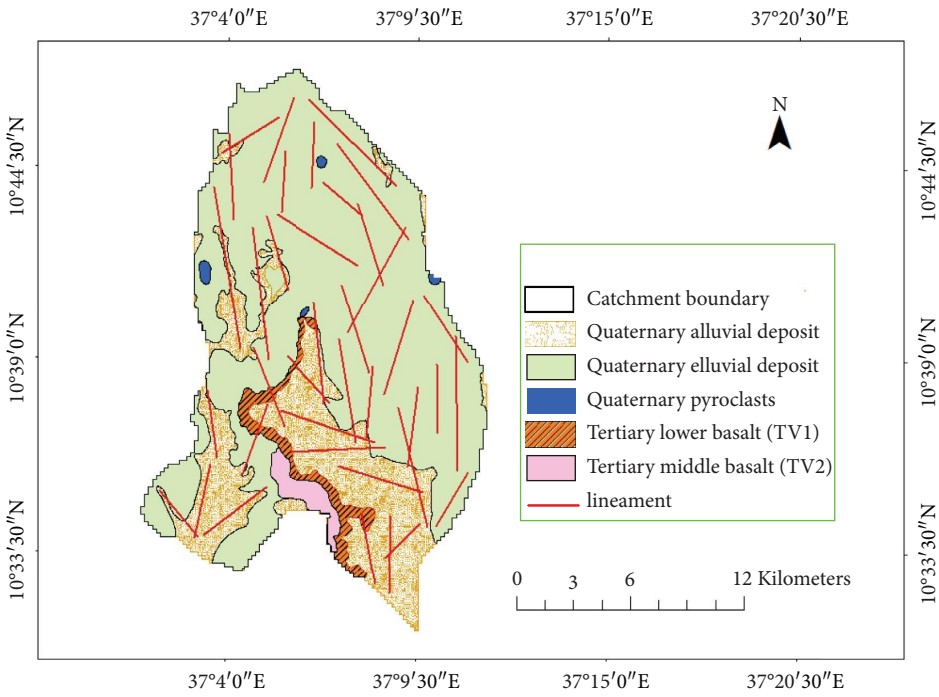

Figure 3: Geological map of the study area.

2.6. Materials

2.6.1. Water Sample Collections. A hydrocensus of the study area was conducted before the sample collection. This study was performed during the first field visit in March 2020. This helped identify sampling points for systematic hydrogeochemical and cluster analyses [29]. During the hydrocensus, the number of water wells, whether springs were accessible, and whether they were productive were taken into account. During the second field visit, water samples and measurements were taken simultaneously to meet the goals of the study. For the groundwater chemistry study, the sampling point was chosen based on differences in geological formation, geomorphology, land use pattern, population density, and other factors.

After pumping for approximately 10 min to obtain fresh water from the ground, samples were taken from 26 places where people usually obtain water to drink or use for irrigation. After pumping for approximately 10 min to obtain fresh water from the ground, samples were taken from 26 places where people usually obtain water to drink or use for irrigation. In addition, the absolute location of each water point was recorded using GPS. The samples were collected and sealed securely using a one-liter plastic bottle after washing the device (plastic bottles and its caps) as often as required with the water to be tested to avoid mixing the water if it was left in the bottle before sampling and to eliminate other common, undesirable items. The samples were taken in April 2020 during the dry season using standard methods of the sampling protocol [30]. The collected samples were protected from direct sunlight during transportation to the laboratory and transported within four days. The pH, total dissolved solids (TDS), and electrical conductivity (EC) were measured on-site using multiple-parameter portable water analyzer kits (HANNA, HI 991301), which were calibrated before use and checked against a reference solution at each station. To determine the temperature, a mercury thermometer was placed in water sufficiently long to reach equilibrium.

2.7. Methods

2.7.1. Data Analysis. Groundwater samples were collected as per guidelines [30]. Ca^{2+}, Mg^{2+}, and Fe^{2+} concentrations were determined using atomic absorption spectrophotometry. Using flame photometer emission and absorption techniques, the amounts of Na^{+} and K^{+} were measured. PO_4^2, $^{-}F^{-}$, NO_3^-, and Cl^- concentrations were measured using the colorimetric technique. HCO_3^-, CO_3^{2-}, and SO_4^{2-}, ions were measured using sulfuric acid titration procedures. However, CO_3^{2-} was not identified in any of the samples.

2.7.2. Hydrochemical Data Reliability Check. Depending on the electroneutrality condition, the total of positive and negative charges in water was used to calculate the accuracy of the analysis for primary ions using the following equation [8]:

$$\text{Electroneutrality\%} = \left[\frac{\sum \text{of cations} - \sum \text{of anions}}{\sum \text{of cations} + \sum \text{of anions}}\right] \times 100. \quad (1)$$

where cations and anions are expressed as meq/l. The sums are taken over the cations Na^+, K^+, Mg^{2+}, and Ca^{2+} and anions Cl^-, HCO_3^-, and SO_4^{2-}. The remaining analyzed chemical parameters were excluded because their concentrations were low. Consequently, their incorporation in the calculations had a negligible impact on charge balance error (CBE) values, and consequently, CBE values were based on main ion concentrations [31]. The CBE threshold of ±10% was selected [11, 32].

2.8. Methods for Multivariate Statistical Analysis

2.8.1. Data Preparation for Multivariate Statistical Analysis. Almost all geoscientific data require statistical analysis to evaluate their dependability and error rates [33]. Multivariate statistical analysis, which permits the classification of separate groups of groundwater samples and the determination of the association between chemical characteristics and groundwater samples, can be used to classify groundwater [11]. Multiple correlations are employed in statistics to demonstrate the degree of connection between geochemical variables. Consequently, it is simpler to identify the relevant hydrogeochemical facies [34].

A multiple correlation analysis was conducted using all tested (Physicochemical) parameters from the study area. Based on the correlation coefficient (r), the degree of relationship between these parameters was defined as very high (if $r = 0.8$ to 1.0), high (if $r = 0.6$ to 0.8), and low (if r 0.6) [35]. The correlation coefficient (r) between variables was measured using IMBSPSS V.23 software [36].

IBM SPSS was used to perform R-mode and Q-mode hierarchical cluster analyses (HCA) as well as R-mode factor analyses in principal components (RFA). The data were subjected to a multivariate statistical analysis using the method given by [11]. The dataset used in the present study constituted a data matrix of 26 sampling sites (observations) by 12 parameters (variables). As suggested by [37], a few parameters were excluded from the analysis: pH and temperature are additive characteristic parameters. Thus, 12 selected parameters include the major and minor constituents Ca^{2+}, Mg^{2+}, Na^+, K^+, HCO_3^-, Cl^-, NO_3^-, F^-, PO_4^{2-}, SO_4^{2-}, TDS, and EC were chosen. All selected parameters, except F^- and SO_4^{2-}, are substantially positively skewed, and their frequency distribution in mg/L is not regular. Except for F^- and SO_4^{2-}, all chemical parameters were log-transformed. Using equation (2) converted all of these variables to standard scores (Z_i).

$$Z_i = \frac{(xi - x)}{S}, \quad (2)$$

where Z = standard score of sample i, xi = value of sample i, x = mean, and s = standard deviation.

2.8.2. Methods for Hierarchical Cluster Analysis. Typically, hydrogeochemical data are categorized using the hierarchical cluster analysis (HCA), a widely utilized clustering method [14]. Determining the appropriate linkage rule and similarity measurement combination is one of the critical decisions in performing HCA [38]. It was determined that the square Euclidean distance (Q-mode HCA) or the square Euclidean distance (R-mode HCA) would be used as the distance or similarity measure between sampling sites and parameters, paired with Ward's method as a linkage rule, which merges clusters according to the sum of squares criterion for minimum information loss. According to [11], the groups that employ square Euclidean distance as the similarity measure and Ward's approach as the connection rule are the most distinctive. To create a tree diagram or dendrogram, a study of the similarity between observations/parameters is conducted [11]. Consequently, the dendrogram can be visually studied in order to cluster samples. Reference [11] provide a thorough overview of the benefits and applications of the HCA in hydrogeochemistry, as well as the mathematical derivation underlying the HCA.

2.8.3. Methods for Principal Component Analysis. Reference [11] studied the interaction among groundwater quality measures and found the processes that govern the variability of groundwater quality using the principal component analysis. Using the R-mode factor analysis, samples are categorized according to their parameters in this manner (RFA). The R-mode factor analysis is highly effective in studies of groundwater quality and has various advantageous properties that ease data interoperability [34]. The primary goal of the principal component analysis is to minimize the dimensionality of multivariate information [39].

The eigenvalue, percentage of cumulative variance, and component loading scores are the important functions of PCA analysis [34]. The Kaiser criterion and the scree plot with the varimax rotation method were used to determine the optimum number of components, as suggested by [39]. The Kaiser criterion eliminates the principal components with eigenvalues smaller than one.

2.9. Hydrogeochemical Processes. For hydrogeochemical process assessment in the study area, groundwater, Gibbs diagram, piper plot, interionic relationships, and statistical results were employed.

2.10. Methods for Water Quality Evaluation

2.10.1. Water Quality Index (WQI). Numerous metrics, including Na^+, K^+, Ca^{2+}, Mg^{2+}, HCO_3^-, Cl^-, SO_4^{2-}, F^-, pH,

EC, TDS, and TH, are essential for most studies on the development of the water quality index [40]. The study employed the water quality index (WQI) and considered one of the most reliable methods for measuring the contamination level in groundwater to determine if water is appropriate for drinking [41]. The WQI is measured on a scale from 0 to 300, with lower values signifying higher water quality [41].

In the present study, the WQI was calculated in four steps, which are as follows:

Step 1. The 15 drinking water quality characteristics have been assigned weights (wi) based on their relative relevance. Parameters substantially affecting water quality were awarded the greatest weight, 5. Due to their significance, TDS, NO_3^-, and F^- were given the most weight in the evaluation of water quality [42]. The remaining parameters were assigned a weight between 2 and 4 based on their importance to the overall water quality.

Step 2. Relative weight was computed using the following equation:

$$\mathrm{Wi} = \frac{\mathrm{wi}}{\sum_i^n wi}. \tag{3}$$

Wi represents the relative weight of each sampled parameter, whereas wi represents the weight of each parameter, respectively. n represents the number of parameters in total.

Step 3. As recommended by [43], each parameter's quality rating scale (Qi) was calculated by dividing its amount by the respective standard and multiplying it by 100 (equation (4)).

$$Qi = \frac{\mathrm{Ci} \times 100}{\mathrm{Si}}. \tag{4}$$

Qi determines the quality rating, Ci is the concentration of each chemical characteristic in each water sample, and Si is the [43] established drinking water standard.

Step 4. First, subindices (SI) were calculated for each chemical parameter, and then, equation (5) was used to get the WQI.:

$$\mathrm{SI}_i = \mathrm{Wi} \times \mathrm{Qi}. \tag{5}$$

$\mathrm{SI_i}$ is the subindex for the i^{th} parameter, Wi is the relative weight for each parameter, and Qi is the score based on the i^{th} parameter's concentration. As seen by equation (6), the overall water quality index (WQI) is computed by adding the subindex values (SI_i) for each groundwater sample.

$$\mathrm{WQI} = \sum \mathrm{SIi}. \tag{6}$$

2.11. Irrigation Water Quality Indices. Several criteria were utilized to assess the appropriateness of groundwater for irrigation in the research area. Sodicity hazard was measured using SAR and Na%, whereas salinity hazard was measured using EC and TDS. Additionally, the RSC, MH, and PI were examined. This study's methodology is depicted in Figure 4 as a flowchart.

3. Results and Discussion

3.1. Evaluation of Physicochemical Parameters

3.1.1. Temperature. Concerning water quality, a critical aspect of water temperature is the influence it has on dissolved gases. As the water temperature increases, the solubility of the gas decreases, and water holds fewer gases. Temperature also impacts alkalinity, salinity, and electrical conductivity [44]. The average annual atmospheric temperature in the study region is 20 degrees Celsius. The research area's minimum, maximum, and average groundwater temperatures are 20°, 24°, and 22.47°, respectively.

3.1.2. Hydrogen Ion Activity (pH). pH can be defined as the negative logarithm to base ten of the concentration of hydrogen ions in a solution. The measurement of hydrogen ions (H^+) is made using this parameter. Water molecules break down into H^+ and OH^- (hydroxyl) ions in the natural world. There is a direct correlation between the pH of the water and the mobility and solubility of many compounds. It is important to note that only a few ions, such as sodium, potassium, nitrate, and chloride, remain in solution throughout the pH range in groundwater. Most metallic elements are soluble as cations in acidic groundwater; however, when the pH is raised, they precipitate as hydroxides or basic salts [45].

The study area's minimum, maximum, and average pH values were 6.34, 7.83, and 7.1, respectively. The pH levels in the study area groundwater tend to decrease toward the deep groundwater due to the dissociation of silicate minerals resulting in a high concentration of HCO_3^- and H^+ that leads to a decreased pH value. The maximum value of 7.83 was noted in the spring water (Cs-9), and a minimum value of 6.34 was recorded in the deep borehole (BH-2). According to [46], a pH greater than 8.2 suggests the existence of carbonate ions. Bicarbonate ions are determined if the pH is 8.2. Most bicarbonate ions are transformed into carbonic acid molecules at pH levels below 4.5. Based on the pH values of the water samples, bicarbonate ions (HCO_3^-) dominate the alkalinity in the research area, while carbonate ions (CO_3^-) are almost nonexistent. Figure 5 shows the spatial variability of pH.

3.1.3. Electrical Conductivity (EC). Electric conductivity is the ability of water to conduct an electric current at a particular temperature, and it is often quantified in microsiemens per centimeter (Hem, 1985). It is the overall concentration of soluble salts in water. EC varied from 52.6 μs/cm (HD) to 5430 μs/cm (BH-2) with a mean value of 987.3 μs/cm, as determined by the study. Although the average EC value is within the allowable range, four deep wells exceeded the maximum permissible range of the [43] standard EC value for drinking water, which is 1000 s/cm.

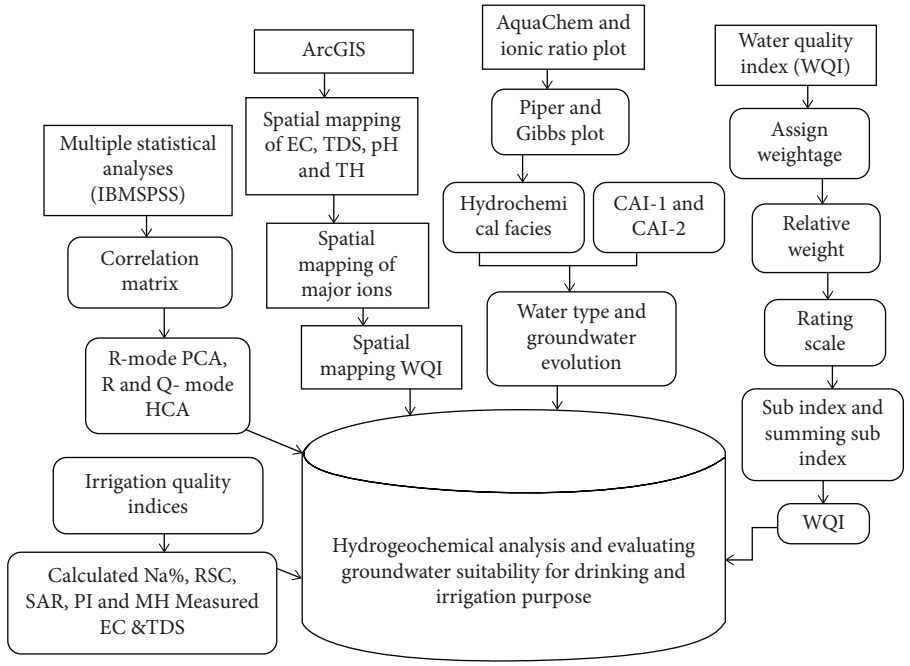

Figure 4: Methodology flow chart.

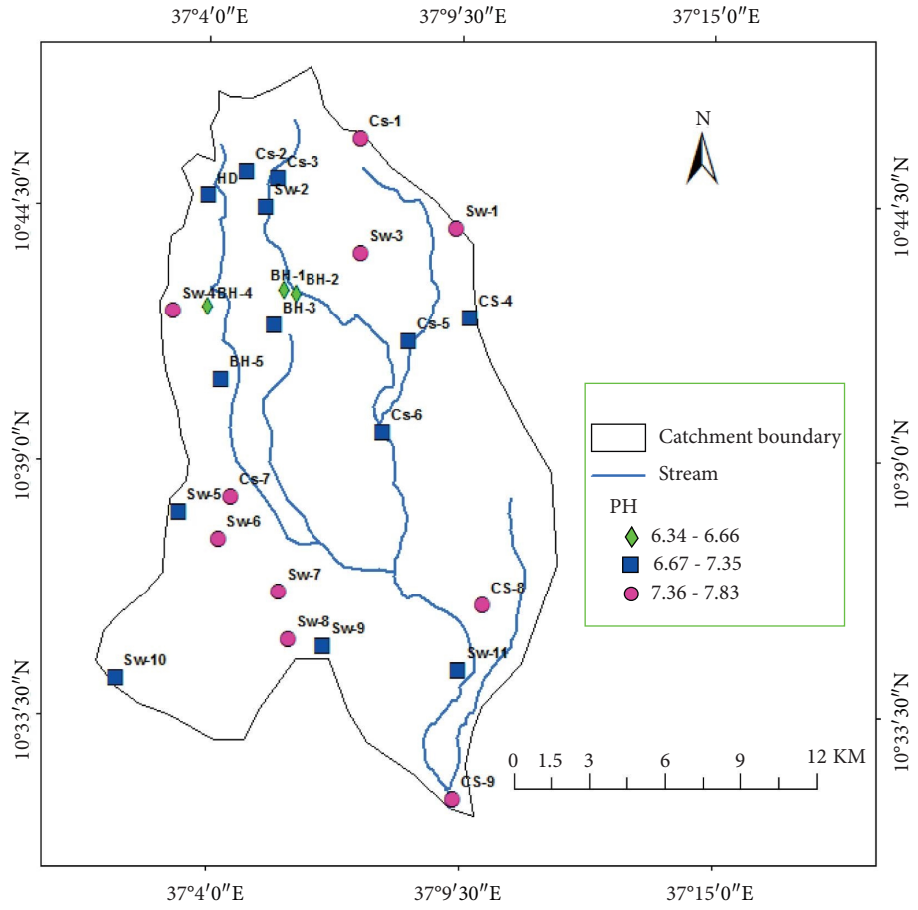

Figure 5: Spatial variability map of pH.

This higher electrical conductivity values indicates that the ground water in the area has leached too much mineral elements from the rocks at which it moves and resides (there is a higher concentration of dissolved solids), and water has stay for a long period of time in the subsurface (depicting the well has regional recharge). Whereas in shallow wells and springs, the EC value ranged from 52.6 μs/cm to 620 μs/cm, which is below the recommended limit set by [43] for drinking use. Figure 6 shows the spatial variability of EC. It indicates low water-rock interaction, high groundwater flow rate, short residence time, and recharge, which is a meteoritic origin. Generally, EC increases from recharge to discharge area and towards depth increment.

3.1.4. Total Dissolved Solids (TDS). The TDS represents the amount of dissolved minerals, salts, metals, cations, and anions in water. This category includes all substances other than pure water (H_2O) and suspended solids that are found in water. It has been discovered that shallow groundwater in recharge areas contains fewer dissolved solids than deeper groundwater in the same system. In contrast, shallow zones in discharge areas have fewer dissolved solids than shallow zones in recharge areas [8]. It is regarded as a general indicator of water quality, and the number of contaminants presents in the groundwater [47].

In the study area, the value of TDS ranged from 78.1 mg/l (Cs-5) to 3555.5 mg/l (BH-2). The high and brackish nature of water (in average 2073.7 mg/l) value of TDS was found in deep wells. In contrast, TDS in shallow groundwater (on average 246.6 mg/l) has been found in the fresh category. Figure 7 shows the spatial variability of TDS. These high TDS values in deep wells indicated that the groundwater in the area had leached too many mineral elements from the rocks at which it moves, and water has stayed for a long time in the subsurface (depicting the wells as regional recharge). Low (freshwater type) in shallow groundwater is an indicator of low water-rock interaction, high groundwater flow rate, short residence time and recharge is the meteoritic origin.

3.1.5. Hardness. Reference [48] defined hardness as the ability of water to precipitate soap. Generally, it is determined by the presence of calcium and magnesium salts. Reference [8] developed a method of measuring groundwater hardness for residential and industrial purposes. According to Table 1, the hardness of water is classified based on its calcium carbonate concentration.

The average hardness values for deep boreholes, shallow wells, and springs were 726.4, 203.6, and 127.2 mg/l, respectively. Figure 8 shows the spatial variability of total hardness. According to the classification above, most of the groundwater in the area is moderately soft to very hard. Generally, all deep boreholes of the study area are grouped under very hard water. Very high values of local Ca^{2+} and Mg^{2+} concentration in the deep borehole are associated with regional groundwater recharge and have stayed for a long time in the subsurface. In springs and shallow wells, it is due to local variation and dominancy of silicate rocks.

3.2. Major Cations

3.2.1. Sodium (Na^+). Because sodium salts are very soluble in water, all-natural waters include sodium. However, its content in natural waterways fluctuates widely. According to Hem (1985), sixty percent of the Earth's outer crust is formed of feldspar minerals, which are sodium's accessory minerals. When calcium and magnesium in water are swapped for sodium adsorbed to solid aquifer components such as clay minerals, a cation exchange reaction occurs. This causes the water's salt concentration to increase. In the study area, Na^+ values vary widely, ranging from 2.1 mg/l (HD) to 142 mg/l (BH-1). Figure 9 depicts the spatial variability of sodium on a map. In addition to cation exchanges, albite feldspar and clay minerals are the primary sodium sources in the research region's groundwater. The optimal content of Na^+ in drinking water, as determined by the [43], is 200 mg/l.

3.2.2. Potassium (K^+). Due to the strong resilience of rocks containing potassium to weathering, potassium is present in trace amounts in natural streams. Potassium is slightly less prevalent than sodium in igneous rocks, while it is more prevalent in sedimentary rocks (Hem, 1985). In the Yisr river watershed, the concentration of K^+ varied from 0.4 mg/l (HD) to 77.6 mg/l (BH-4), with deep wells (average $K^+ = 29.25$ mg/l) containing a higher level than shallow wells and springs (average $K^+ = 2.5$ mg/l). Figure 10 depicts the regional distribution of potassium. The source of K^+ in the groundwater of the research region is orthoclase feldspars and clays. It was discovered that the average level of K^+ in deep wells exceeded the [43] maximum allowed level of 12 mg/l. This is because, with increasing depth, groundwater undergoes intense water-rock contact, cation exchange, and zonal flow and remains in the subsurface for an extended period.

3.2.3. Calcium (Ca^{2+}). Calcium, the most prevalent alkaline rock, is present in numerous common rock minerals. Numerous igneous rock minerals, including the chain silicates pyroxene, amphibole, and feldspar, include calcium [44]. The average Ca^{2+} concentration in groundwater collected for the study results of the research region ranges from 21.1 mg/l (HD) to 220.5 mg/l (BH-3). The source of calcium in the study area is assumed to be amphibole, plagioclase feldspar, pyroxene, and clay minerals. It was found that calcium concentration in three deep wells (BH-1, BH-3, and BH-4) exceeded the [43] allowable maximum limit (75 mg/l). Due to depth, groundwater experienced profound water-rock interaction, regional flow, and a long time in the subsurface. However, the average value of the overall analyzed sample in the study area is 57 mg/l, which is lower by 23.5 mg/l than [43] allowable maximum limit. Figure 11 shows the spatial variability map of calcium. Generally, shallow wells and springs have lower calcium concentration than deep boreholes, implying less water-rock interaction or rapid groundwater flow rate in shallow wells and springs than deep wells.

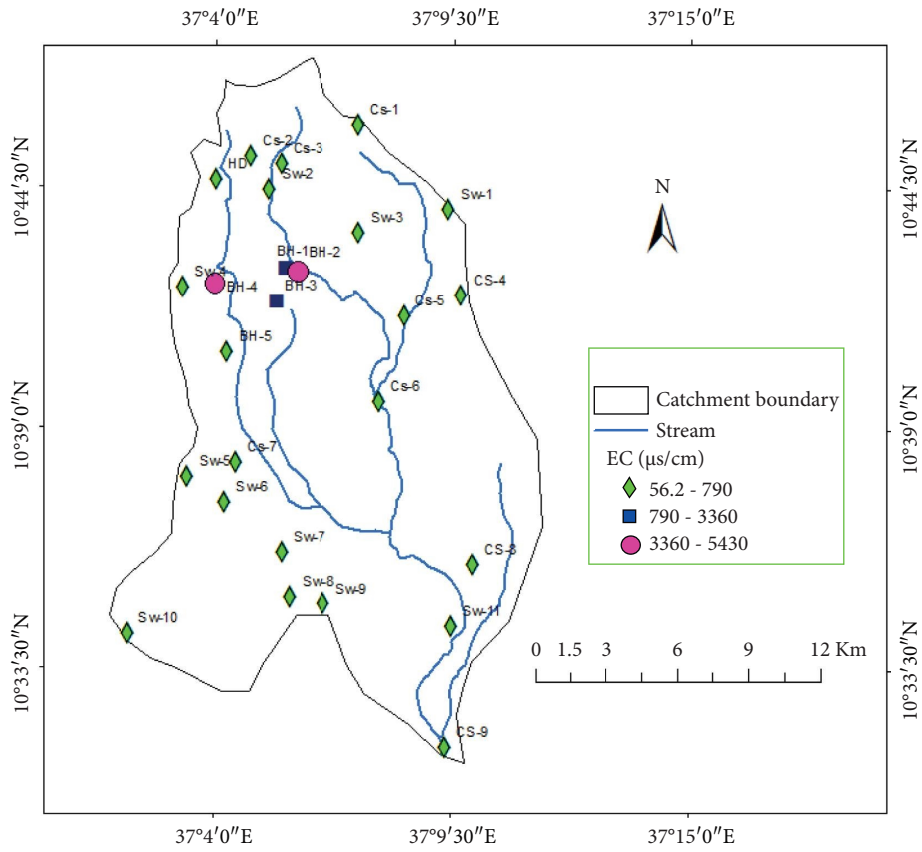

Figure 6: Spatial variability map of EC.

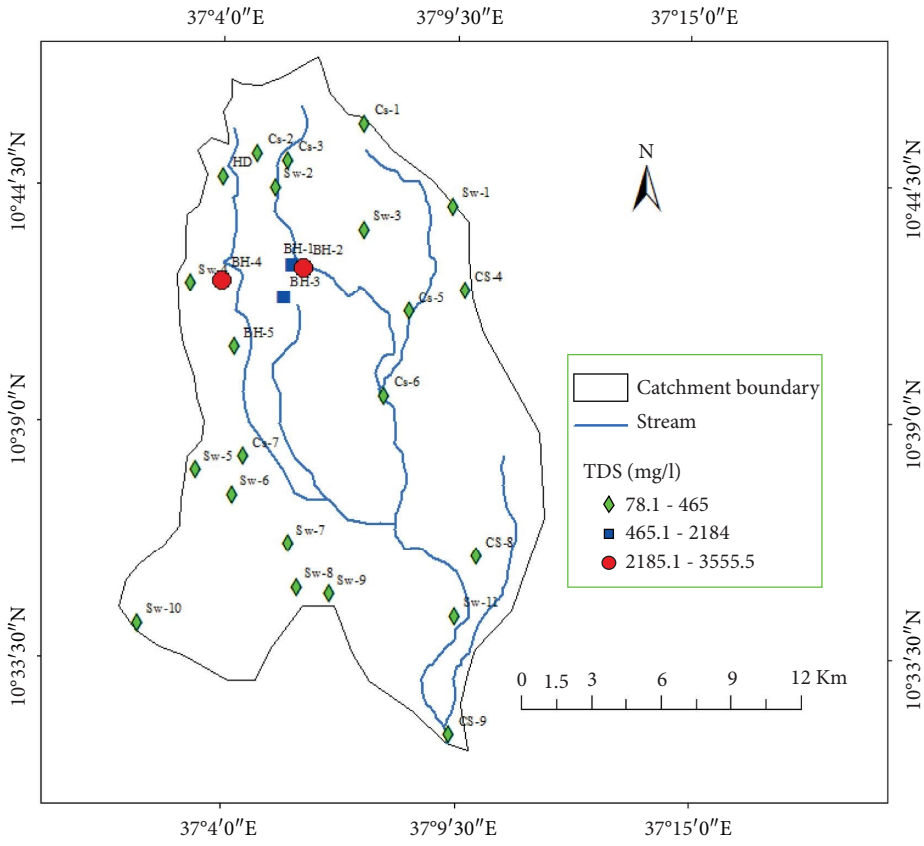

Figure 7: Spatial variability map of TDS.

Table 1: Hardness classification of water [48].

Hardness rating	The concentration of calcium carbonate (mg/l)	Number of samples
Soft	0 to < 75	2
Medium soft	75 to < 150	9
Hard	150 to < 300	9
Very hard	>300	6

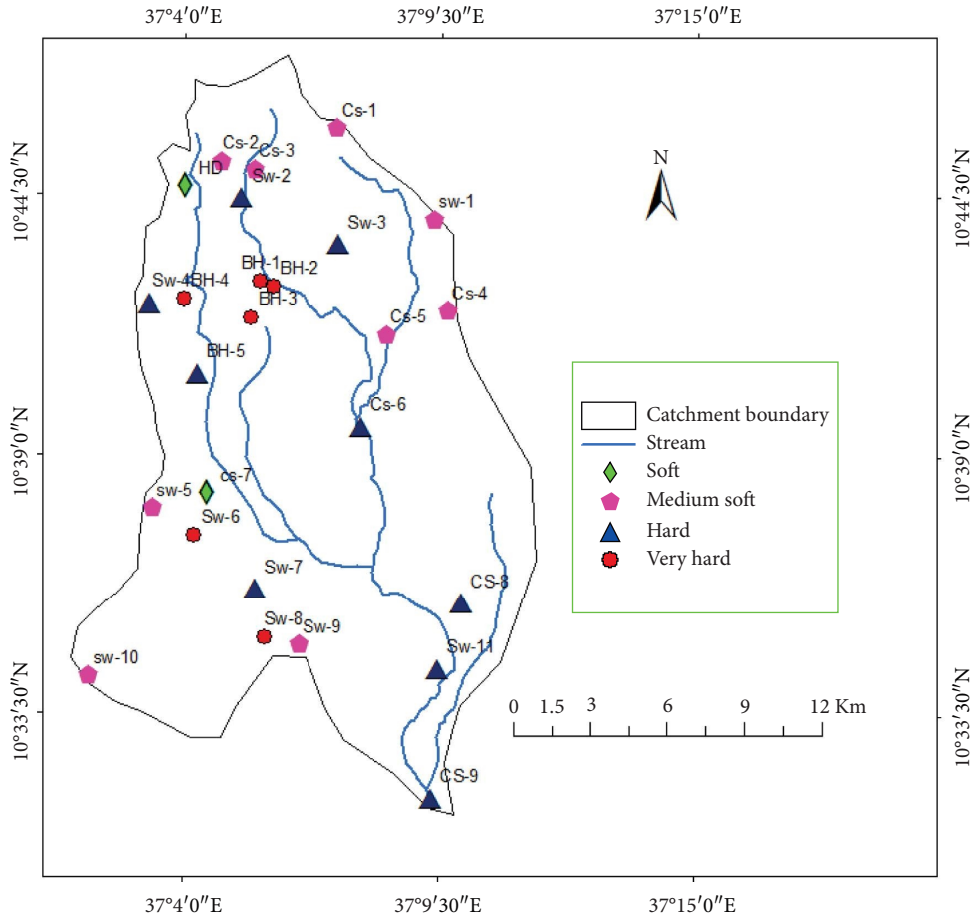

Figure 8: Spatial variability map of hardness.

3.2.4. Magnesium (Mg^{2+}). Magnesium is typically found in the dark-colored ferromagnesian minerals in igneous rocks (Hem, 1985). In the investigated area chemical analysis result of magnesium varied from 2.9 mg/l (HD) to 247.7 mg/l (BH-2). The source of magnesium in the study area groundwater is amphibole, pyroxene, olivine, and clay minerals. Like calcium, magnesium concentration is higher in deep boreholes than in shallow wells and springs. It was found that magnesium concentration exceeded the [43] allowable maximum limit (50 mg/l) by 197 mg/l, 50 mg/l, and 55.3 mg/l for BH-2, BH-1, and BH-4, respectively (Figure 12). This is due to a similar reason given for calcium. The average value of the overall analyzed sample in the study area is 37.3 mg/l, which is lower by 12.7 mg/l from [43] allowable maximum limit. Figure 12 shows the spatial variability map of magnesium.

3.3. Major Anions

3.3.1. Chloride (Cl^-). Because of their high solubility, chlorides have a tremendous capacity for migration. Chloride is not a typical mineral component, and chlorine is much more likely to be found due to pollution [44]. In the investigated area, the concentration of Cl^- ranged from 0.71 mg/l (Cs-1) to 40.3 mg/l (Sw-8) (Figure 13). Generally, high chloride concentration was found in most shallow wells and springs than in deep wells indicating anthropogenic sources associated with some pockets of an agricultural activity dominant area. According to [43], the maximum recommended chloride limit for drinking is 250 mg/l. Accordingly, the study area's groundwater chloride concentration was within the recommended limit.

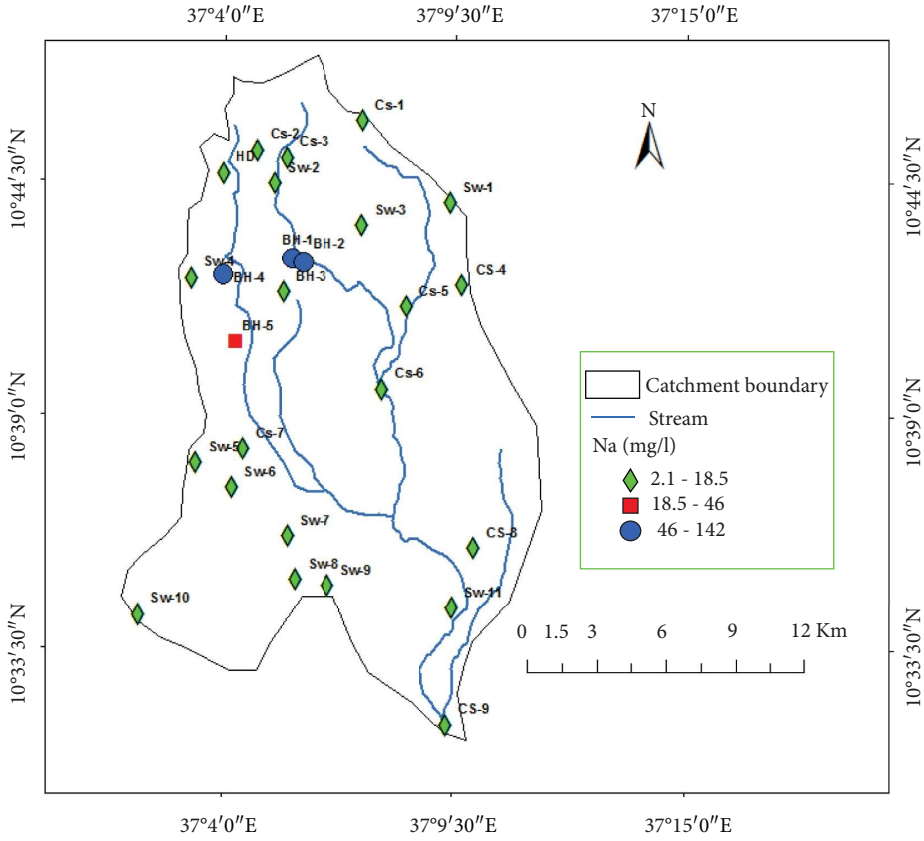

Figure 9: Spatial variability map of sodium.

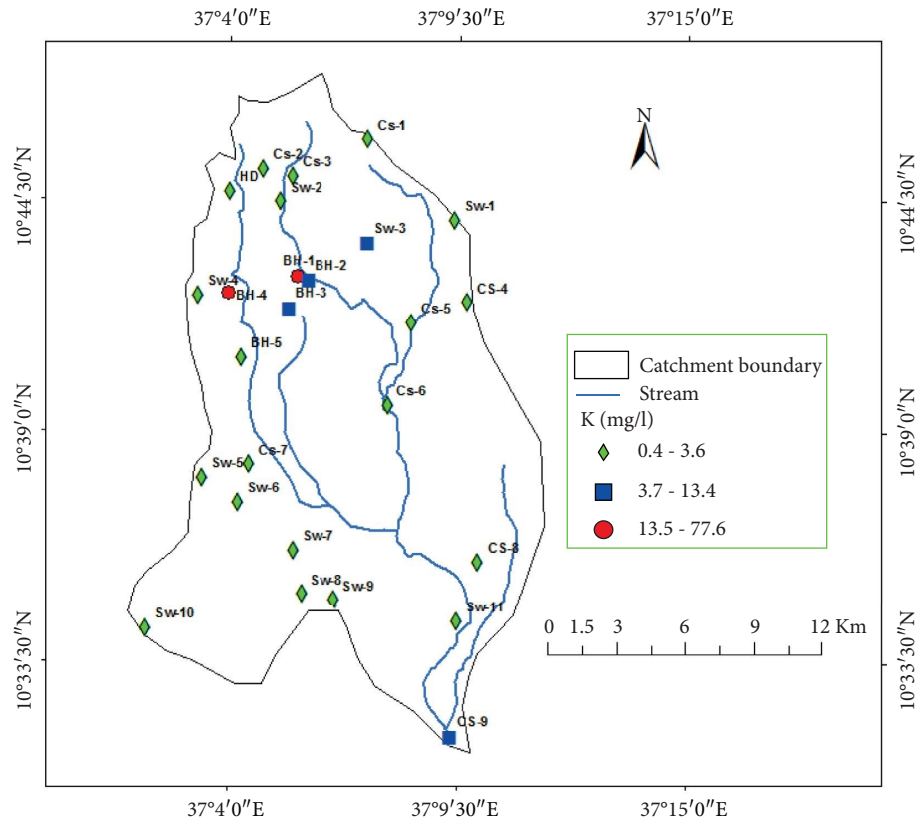

Figure 10: Spatial variability map of potassium.

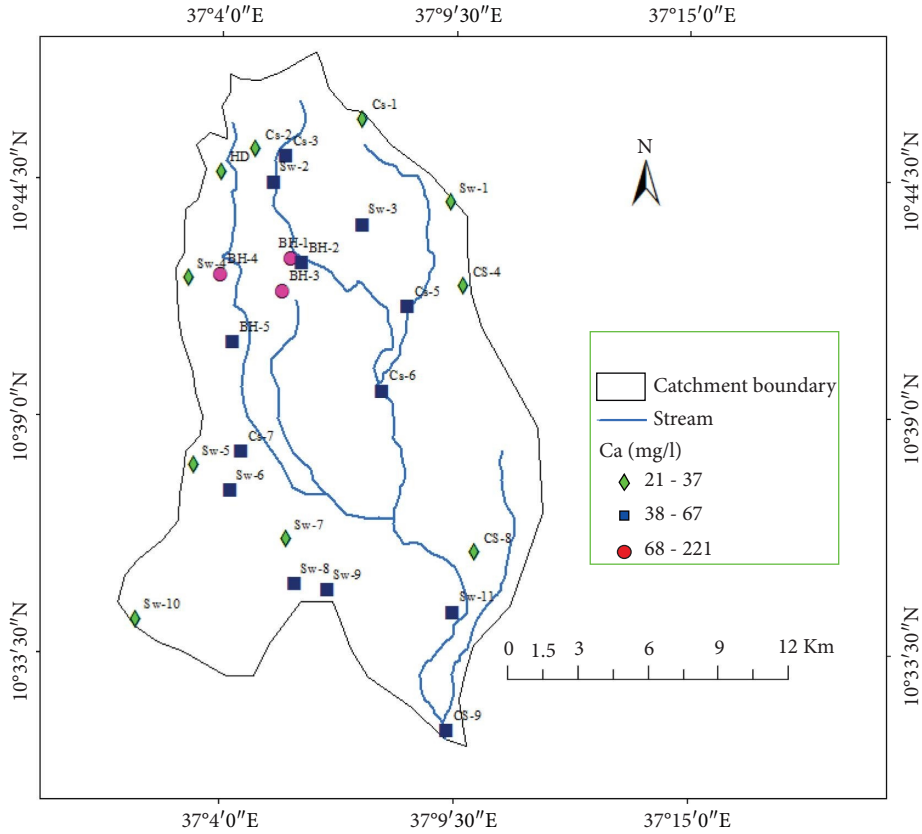

Figure 11: Spatial variability map of calcium.

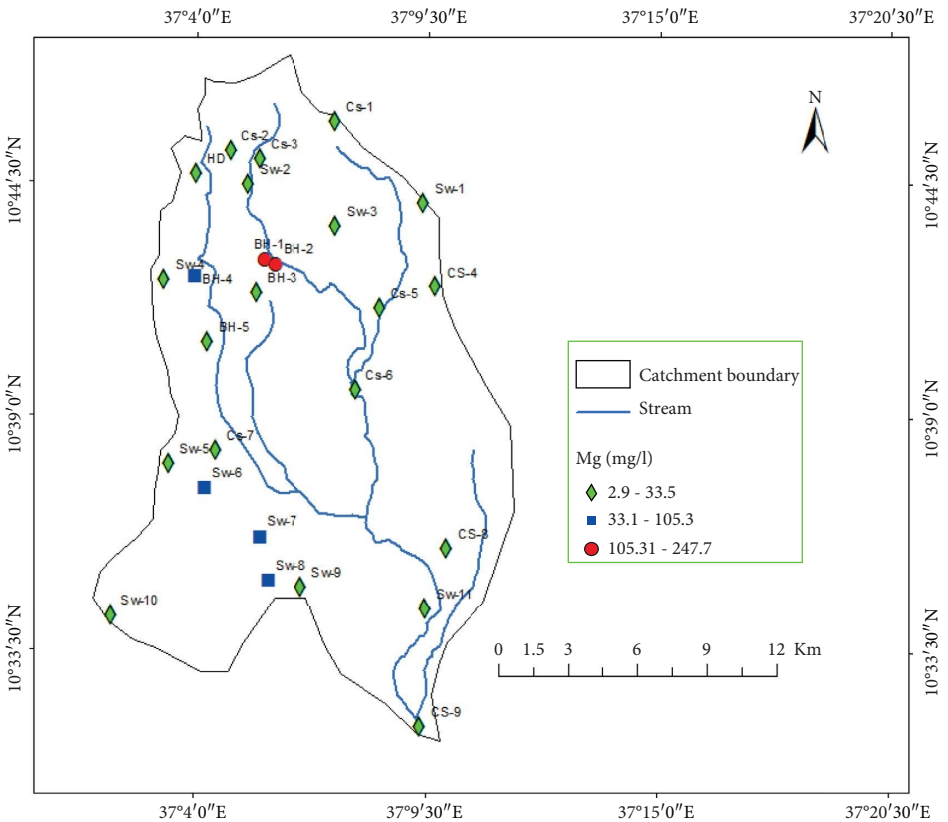

Figure 12: Spatial variability map of magnesium.

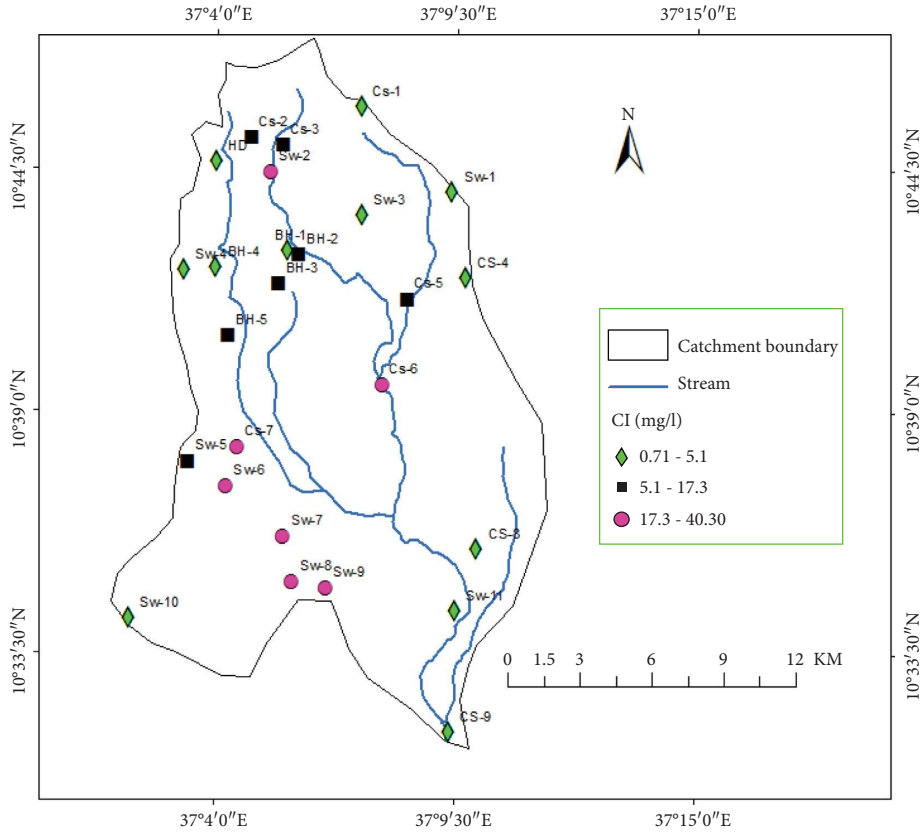

Figure 13: Spatial variability map of chloride.

3.3.2. Sulphate (SO_4^{2-}). The sulfate concentrations in the examined area varied from 0.1 mg/l at Sw-3 to 14.3 mg/l at Sw-11, as determined by water analysis. Based on the findings of this investigation, the optimal content of sulfate in the study area was determined to be within the [43] recommended limit of 250 mg sulfate per liter for drinking. The absence of host rocks causes a low sulfate concentration (sedimentary rocks such as gypsum).

3.3.3. Bicarbonate (HCO_3^-). Carbonate has an effect on the hardness of water. HCO_3^- is predominantly derived through the dissolution of carbonate rocks, such as dolomite, limestone, and magnesite, resulting in the precipitation of bicarbonate. Since there is no carbonate in the area of research, the high proportion of bicarbonate origin amongst anions is not due to carbonated dissolution. Therefore, the source of bicarbonate ions is hydrolysis from dominant silicate minerals in the study area and meteoritic waters. In the study area, the analyzed minimum, maximum, and average concentrations of bicarbonate have found 75 mg/l, 1985 mg/l, and 471.9 mg/l, respectively (Figure 14). The high value of bicarbonate was indicated in deep boreholes than shallow groundwaters testifie to more HCO_3^- ions precipitated by hydrolysis of silicate minerals along with depth increments.

According to [2], the high concentration of bicarbonate in volcanic rock is principally due to the incongruent hydrolysis of silicate minerals by the following reaction:

$$\text{Rocks} + H_2CO_3 \longrightarrow \text{cations} + H_4SiO_2 + HCO_3 + \text{solids}.$$

The highest acceptable quantity of HCO_3^- in drinking water, as established by the US public health agency (WHO criteria are unavailable), is 120 mg/l. However, the average bicarbonate value in the research area exceeds the US Public Health Service's prescribed levels for drinking water, indicating that substantial silicate hydrolysis has occurred in this region. In addition, it suggests that the study area is situated within the recharging zone.

3.3.4. Nitrate (NO_3^-). Land drainage and plant and animal detritus are natural nitrate sources in water. Reference [49] noted that leachates from waste disposal facilities and sanitary landfills may add to the natural concentration. Given that most of the research area relies largely on agriculture, the nitrate concentration of groundwater was given special consideration. According to [45], crop fertilization is the most significant agricultural technique contributing to nitrate pollution of unconfined shallow groundwater. The average value across all samples studied was 8.94 mg/l. [43] recommended a maximum drinking concentration of 50 mg/l. Hence, the contamination levels are usually below the prescribed level, except for one well (Sw-1), where nitrate levels were found to be 55.4 mg/l due to a nearby latrine and a pocket of significant agricultural fertilizer inputs (Figure 15). In recent years, groundwater NO_3^- concentrations are often greater in shallow

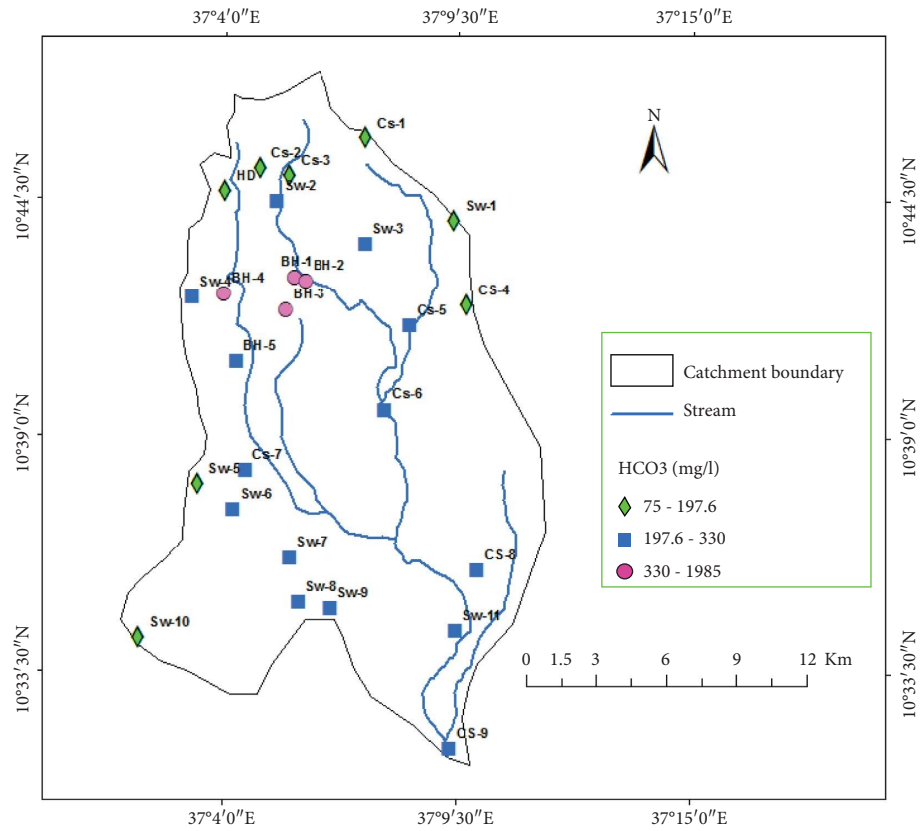

Figure 14: Spatial variability map of bicarbonate.

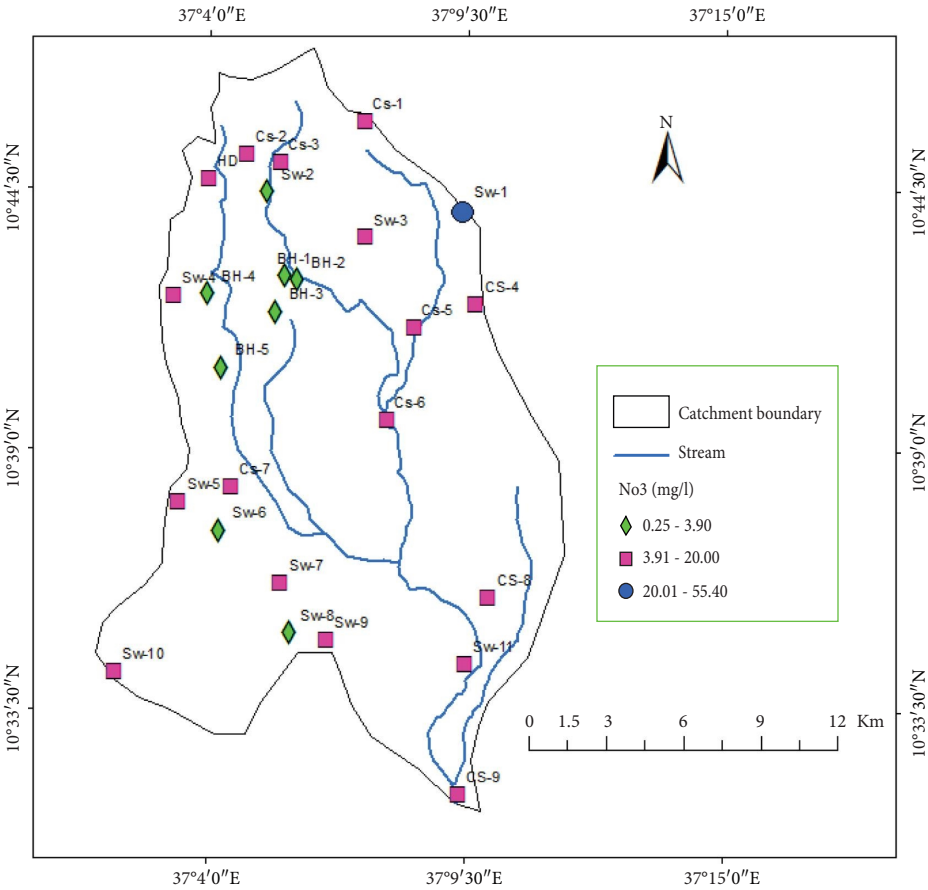

Figure 15: Spatial variability map of nitrate.

groundwater systems than in deep groundwater systems, implying a rise in shallow groundwater contamination.

3.4. Graphical Presentation and Hydrogeochemical Facies. Hydrochemical facies are defined by [8] as distinct zones of cation and anion levels. Hydrology, solution kinetics, and flow patterns influence an aquifer's hydrogeochemical facies. Utilizing hydrochemical diagrams aids in the detection of groundwater system evolution tendencies. Box and Whisker, Schoeller, and Piper diagrams have been used to acquire a more profound knowledge of the development and facies of the hydrogeochemical variables of groundwater in this study region.

3.4.1. Piper Diagram. In a Piper trilinear diagram, the proportion of cations and anions was displayed on distinct triangular graphs (Figure 16). By intersecting the lines between the two sample points on the triangle graph and the diamond-shaped graph in the center, we can compute the proportion of the primary ion composition. From the Piper trilinear diagram, one can observe that the cations plot mainly clustered around the calcium and magnesium ion implies that the dominant cations are calcium and magnesium, with some samples aligned towards the sodium ion apex in deeper groundwater showing progressively increasing sodium enrichment from shallow to deep groundwater. In this case, groundwater carries more ions with increasing depth, and water-rock interaction is dominant. The higher concentration of calcium and magnesium is mainly controlled by the hydrolysis of silicate minerals, which are dominant in the study area. The anion plots exclusively clustered around the HCO_3^- manifesting that all the water samples are bicarbonate type implies the study area is in a recharge zone and incongruently weathering and hydrolysis of silicate mineral that can be aggravated by dissolved CO_2 existed from the atmosphere and the soils in the area. Generally, the major ionic data plotted on the above Piper's diagram indicated that exclusively all groundwater samples have belonged to Ca-HCO3 type water.

3.4.2. Box and Whisker Diagram. Parametric-based Box and Whisker diagram is another hydrochemical representation method that provides more information to display a statistical summary of any measured database parameter(s). From this diagram (Figure 17), it is represented that the geochemistry of groundwater in the investigated area displays in descending order of $Ca^{2+} > Mg^{2+} > Na^+ > K^+$ and $HCO_3^- > Cl^- > SO_4^{2-} > NO_3^- > F^-$ trend for cations and anions, respectively. Also, from the results it is observed that alkaline earth (Mg^{2+} and Ca^{2+}) are higher than the alkalis (Na^+ and K^+). The abundance of the alkaline earth elements is attributed to the dissolution of Ca^{2+} and Mg^{2+} rich dominant silicate minerals in the aquifer matrix of the study area. From an anion point of view, weak acids (HCO_3^-) exceed the strong acids (Cl^- and SO_4^{2-}) though carbonate (CO_3^{2-}) ions are nil in the groundwater of the study area, portrayed the groundwater in the study area is in recharge zone in addition to hydrolysis of silicate minerals.

The region under investigation predominantly comprises basalt, pyroclastic material pockets, and their sedimentary derivatives. Therefore, Mg^{2+} and Ca^{2+} are expected to be released during weathering reactions of these rocks by recharged water. Thus, the source of Ca^{2+} has assumed amphibole, plagioclase feldspar, pyroxene, and clay minerals, whereas the source of Mg^{2+} is amphibole, pyroxene, olivine, and clay minerals. While the source of Na^+ has assumed feldspar (albite) and clay minerals, and the source of K^+ is orthoclase feldspars and clays, which are dominant minerals in the study area. In terms of anion, the higher concentration of HCO_3^- is derived from silicate hydrolysis. Reference [2] supported that except in Tigray, all highland volcanic rock of Ethiopia is dominated by this ion and is controlled principally by as follows:

(i) In shallow groundwater conditions, the abundant (HCO_3^-) source is atmospheric CO_2^- which reacts with groundwater and is oxidized by organic matter to form dissolved carbon dioxide, elevating the bicarbonate ions.

$$CO_2\ (aq) + H_2O \longrightarrow HCO_3 + H$$

(ii) With depth increments higher concentration of bicarbonates controlled principally by the silicate hydrolysis of the rock minerals and the incongruent reactions.

$$\text{Rocks} + H_2CO_3 \longrightarrow \text{cations} + H_4SiO_2 + HCO_3 + \text{solids}$$

From the natural occurrence of inorganic chemicals point of view, almost all highland volcanic province groundwater of Ethiopia is dominated by Ca^{2+}, Mg^{2+}, and HCO_3^- ions [2, 7], and the dominant water type in the study area confirmed this since the study area is the part of the northwestern highland volcanic province of the country.

3.5. Groundwater Evolution and Chemistry Controlling Mechanism. In general, different chemical processes occur during water interactions with rocks. Minerals found in these rocks will wholly or partially dissolve in water according to the resistance of chemical weathering, which depends on with initial water's disequilibrium with the rocks being contacted. The chemical composition of groundwater is the imprint of the rock-water interaction and chemical processes. So, groundwater chemistry can be used to identify rock-water interactions or chemical processes [50].

Gibbs scattering diagram using TDS vs $(Na + K)/(Na + K + Ca)$ and TDS vs. $Cl/(Cl + HCO_3)$ is used to analyze the effect of hydrogeochemical processes such as precipitation, rock-water interaction, and evaporation on groundwater geochemistry [51]. Hence, most of the analyzed groundwater samples fall around the water and rock interaction domain (Figure 18), suggesting that the major impact responsible for groundwater chemistry in the study area is rock and water interaction (rock weathering dominancy took place) for the hydrogeochemical facies evolution.

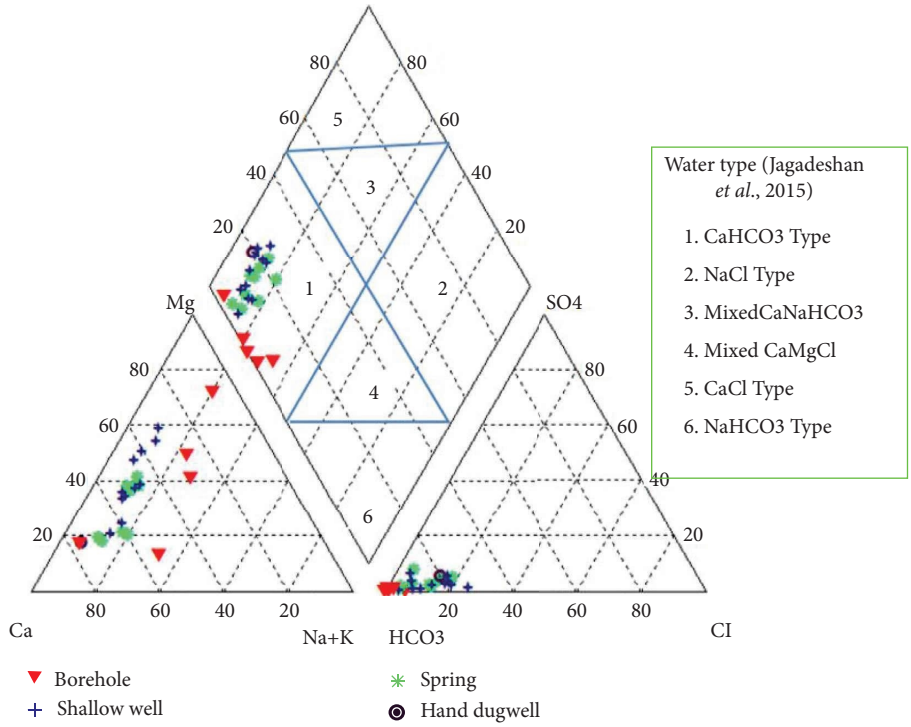

Figure 16: Piper trilinear diagram representation of major ionic (in percent of meq/l) data.

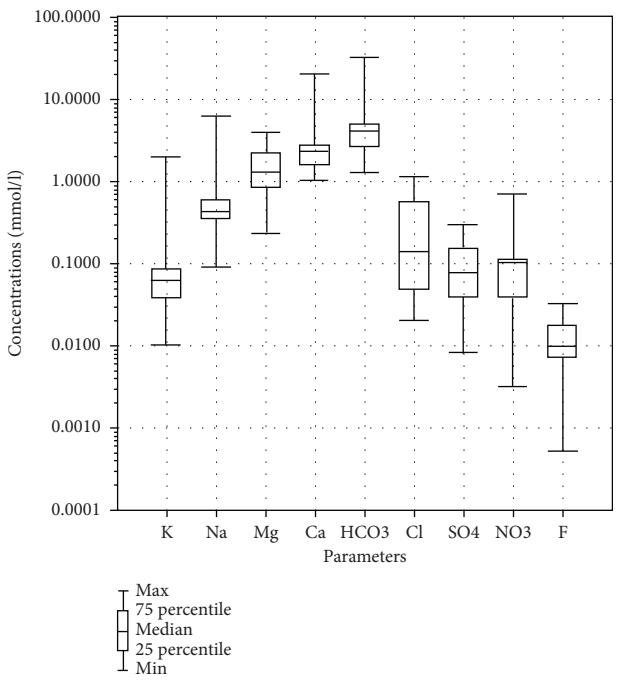

Figure 17: Box and whisker diagram represents the hydrogeochemical trend.

It is confirmed by the principal component (Factor 1) had strong loadings on Na^+, Ca^{2+}, K^+, Mg^{2+}, HCO_3^-, EC, and TDS. These factors were related to mineral precipitation and can be described by the water-rock interaction factor [52].

As the study area is part of the northwestern highland volcanic terrain of the country, all samples (100%) in the study area were found to be dominated by the Ca-HCO_3 groundwater type. Therefore, it confirmed that the high Ca^{2+}, HCO_3^- concentration in the highland volcanic terrain of Ethiopia originated from hydrolysis from basic volcanic and basaltic aquifer [53]. Additionally, ionic ratios and their correlations can be utilized to identify the source of dissolved constituents in the groundwater of the study area. The chemical data of the groundwater samples are plotted for $Na^+ + K^+$ and $Ca^{2+} + Mg^{2+}$ vs. TSC (total sum of cation) (Figures 19(a) and 19(b)). The graphs showed that most of the samples were far above the theoretical line (1 : 1), indicating supply of cations via ion exchange or silicate weathering is more significant [54, 55].

In cation exchange reactions, a high concentration of Na^+ relative to Cl^- or the depletion of Na^+ relative to Cl- is evident [39]. Besides, if the ionic ratio of sodium to chloride is (Na/Cl) > 1, it indicates the presence of another source of Na^+ rather than halite [55] Na^+ containing fertilizer and hydrolysis of silicate rocks released Na^+ to groundwater [55]. Accordingly, the source of the higher concentration of Na^+ rather than Cl^- in the study area, in this case, is due to the hydrolysis of Na^+ containing host rocks (silicates) released into groundwater coupled with cation exchange. As shown in (Figure 19(c)), in the study area, most samples (77%) showed Na/cl > 1, the observed average ratio of 9.33 suggesting continuous supply of Na^+ cation via released Na^+ from silicate weathering by hydrolysis and cation exchange in the groundwater systems except very few samples (23%) disclosed Na/Cl < 1. This ratio is extremely associated with hand-dug wells, springs, and shallow wells exposed to anthropogenic pollution. The plot of $SO_4^{2-} + HCO_3^-$ and $Ca^{2+} + Mg^{2+}$ (Figure 19(d)) showed most samples fall above

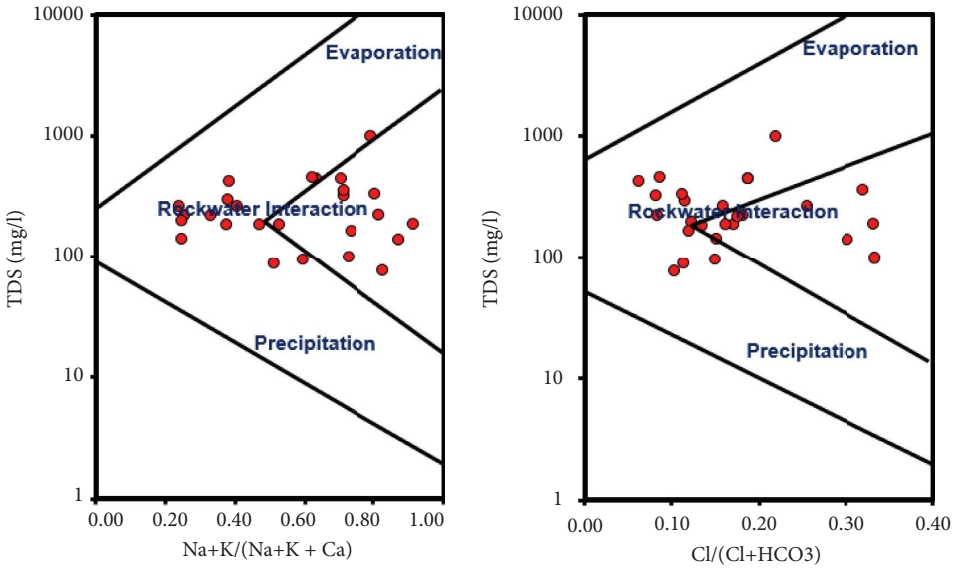

Figure 18: Mechanisms governing groundwater chemistry in the Gibbs diagram.

equiline due to excess bicarbonate, indicating silicate weathering [56] besides, it suggests the presence of ion exchange [57].

In addition, the chloroalkaline indices (CAI) proposed by [58] can be used to validate ion exchange by applying equations (7) and (8) to disclose the hydrogeochemical history of groundwater:

$$\mathrm{CAI}-1 = \mathrm{Cl} - \left(\frac{(\mathrm{Na}^{+} + \mathrm{K}^{+})}{\mathrm{Cl}^{-}}\right) \cdots\cdots\cdots, \tag{7}$$

$$\mathrm{CAI}-2 = \mathrm{Cl} - \left(\frac{\mathrm{Na}^{+} + \mathrm{K}^{+}}{SO4^{2-} + HCO3^{-} + CO3^{2-} + NO3^{-}}\right) \cdots\cdots\cdots \tag{8}$$

According to [58], both indices are negative when there is an exchange between Ca^{2+} and Mg^{2+} in the groundwater with Na^{+} and/or K^{+} in the aquifer material. If there is reverse ion exchange, both index will be positive. In the study area, the calculated indices CAI-1 in about 84.62% of samples ($n = 22$) and CAI-2 in approximately 65.38% of samples ($n = 17$) showed negative indices, which implied exchange of dominant $Ca^{2+} + Mg^{2+}$ in groundwater with $Na^{+} + K^{+}$ in aquifer material/clays thereby increasing Na^{+} and K^{+} concentrations, especially along groundwater flow direction and depth increment.

3.6. Multivariate Statistical Analysis

3.6.1. Correlation Matrix. The correlation matrix of 15 parameters for the 26 groundwater samples in the study area is presented in (Table 2). It shows the linear association between parameters. Good to high correlations between the variables are given in bold. There is a good correlation between EC and Na^{+}, K^{+}, Ca^{2+}, Mg^{2+}, HCO_3^{-}, and TDS. Identically, a good correlation exists between TDS and Na^{+}, K^{+}, Ca^{2+}, $Mg^{2+,}$ and HCO_3^{-}. This correlation implies that TDS is derived from these ions [35]. Poor correlation between Cl^{-} and Na^{+} ($r = -0.14$); K^{+} and Cl^{-} ($r = -0.24$); Na^{+} and SO_4^{2-} ($r = -0.09$), indicating that they are coming from a different source. Very poor correlation between Cl^{-} and Na^{+} ($r = -0.14$); Mg^{2+} and Ca^{2+} ($r = 0.37$) also confirmed that the higher concentration of Na^{+} and $Cl^{-}$and Mg^{2+} and Ca^{2+} in deep boreholes derived from silicate weathering other than halite and carbonate dissolution, respectively.

It is understandable from Table 2 that most of the tested parameters were strongly correlated with HCO_3^{-}. Positively good to high correlation was found between Ca^{2+} and HCO_3^{-} ($r = 0.94$), Mg^{2+} and HCO_3^{-} ($r = 0.79$), and K^{+} and HCO_3^{-} ($r = 0.66$), Na^{+} and HCO_3^{-} ($r = 0.72$) as a result of water-rock interaction, ion exchange, and weathering of the aquifer's initial rocks, HCO3- is now the predominant ion in the aquifer's water chemistry [57]. It is also important to note that poor correlations between NO_3^{-}, PO_4^{-}, Cl^{-}, and SO_4^{2-} with EC (an indicator of mineralization) and all the significant ions indicate the source of these ion's inferences anthropogenic origin. The R-mode HCA result confirms it the dendrogram that NO_3^{-}, PO_4^{-}, Cl^{-} and SO_4^{2-} forming their cluster implies they are derived from an anthropogenic activity rather than geogenic sources.

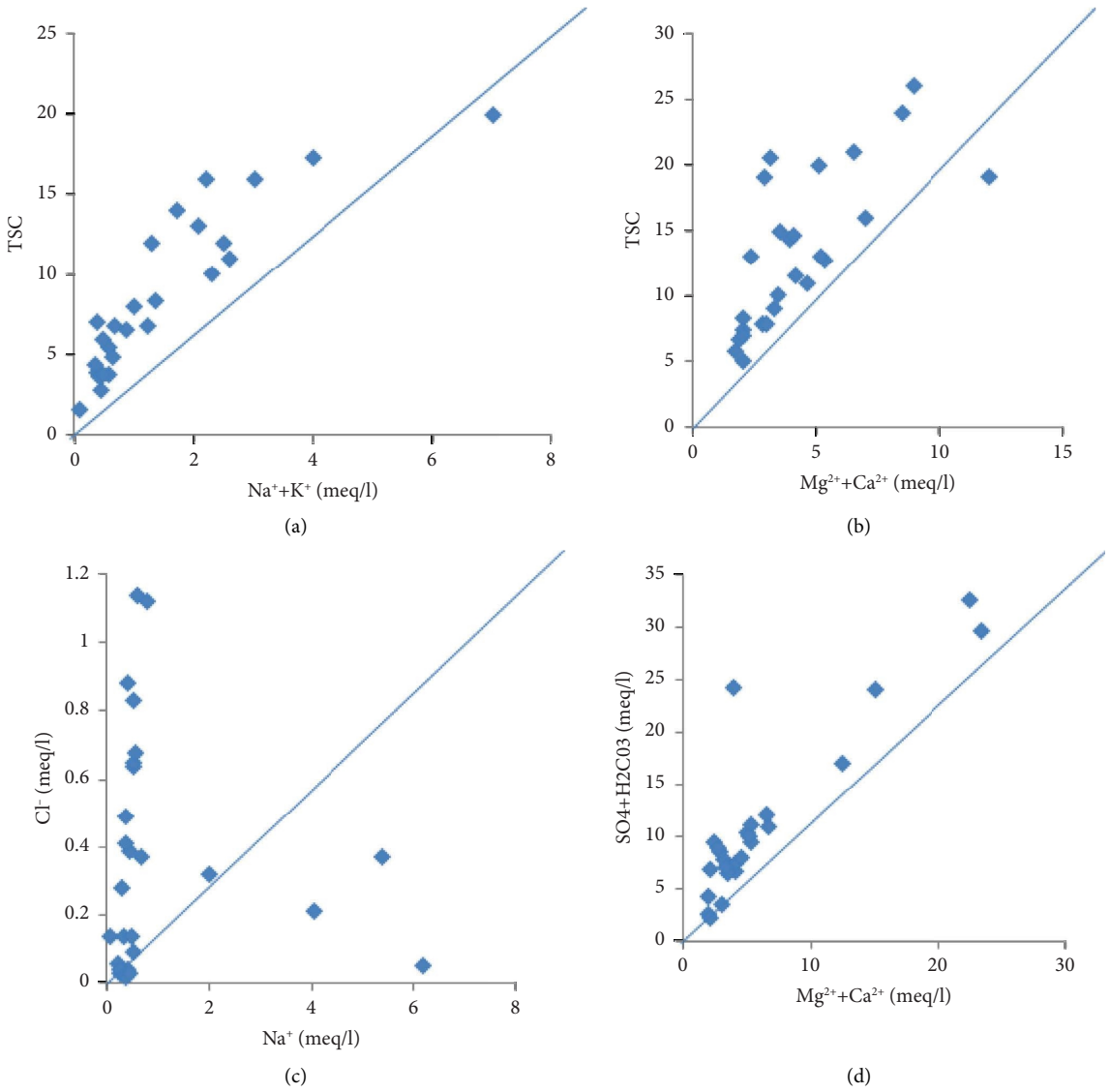

Figure 19: Graphs of different interionic ratios in groundwater of the study area.

Table 2: Correlation matrix of physicochemical parameters.

	pH	EC	Tem	TDS	Na	K	Ca	Mg	Fe	F	Cl	HCO3	No3	So4	PO4
pH	1.00														
EC	**−0.68**	1.00													
Tem	0.13	−0.02	1.00												
TDS	−0.65	**0.97**	−0.03	1.00											
Na	**−0.70**	**0.66**	−0.15	**0.71**	1.00										
K	−0.50	**0.74**	−0.05	**0.70**	**0.72**	1.00									
Ca	−0.28	**0.99**	0.10	**0.90**	**0.93**	0.58	1.00								
Mg	**−0.64**	**0.90**	0.20	**0.89**	**0.54**	0.56	0.37	1.00							
Fe	0.44	−0.15	0.52	−0.11	−0.15	−0.07	−0.08	−0.10	1.00						
F	−0.17	0.44	0.12	0.45	0.35	0.40	**0.60**	0.34	−0.07	1.00					
Cl	0.03	−0.14	0.41	−0.21	−0.14	−0.24	−0.03	0.01	−0.13	0.34	1.00				
HCO3	**−0.67**	**0.99**	−0.01	**0.96**	**0.72**	**0.66**	**0.94**	**0.79**	−0.14	0.49	0.36	1.00			
No3	−0.39	−0.36	−0.10	−0.32	−0.35	−0.27	−0.33	−0.31	0.25	−0.17	0.41	−0.37	1.00		
So4	−0.12	0.08	0.19	0.02	−0.09	0.17	0.18	−0.05	−0.22	0.29	0.43	0.03	−0.23	1.00	
PO4	0.01	0.47	−0.18	0.51	0.30	0.52	0.48	0.23	0.02	0.37	−0.43	0.42	0.38	0.07	1.00

Bold values show the strong correlations between the chemical components.

The temperature has no good correlation with all other parameters. Also, pH has no negatively good correlation with some parameters ($r = -0.68$, -0.52, -0.94, -0.65, -0.64, and -0.67) of EC, TDS, Na^+, K^+, Mg^{2+}, and HCO_3^- respectively, and consequently, temperature and pH have little to no effect on the geochemistry of the water. In contrast, pH is impacted by several factors other than the examined parameters [59].

3.6.2. Hierarchical Cluster Analysis (HCA). To group/cluster the observations or variables of the Yisr river catchment hydrochemical database on their similarity and distinct characteristics, two types of clustering techniques were utilized: Q-mode (Figure 20 to group based on the samples and R-mode (Figure 21) and to group based on different water variables (parameters).

The dendrogram displays the findings of the Q-mode clustering-based hierarchical cluster analysis of 26 groundwater samples from the research locations. In response to a visual examination of the dendrogram, the phenon line might be moved to identify more or fewer groups [11]. The phenon line was picked at a linkage distance of five across the dendrogram, resulting in three clusters. The elevated linkage distance between cluster 3 (25) and the other two clusters indicates that the groundwater samples in cluster 3 are geochemically unique from those in the other two clusters. Most cluster 3 wells are deep groundwater wells, except BH-5, which has a high TDS compared to the other two clusters. Due to the regional flow and the long residence period of the ions, the EC value shows that water and rock have interacted more. Clusters 1 and 2 share the same linkage distance (6.5) and have the highest degree of similarity among all clusters. Therefore, it is anticipated that the geochemistry of the groundwater samples from clusters 1 and 2 will share some similarities [37].

Additionally, significant connections between subclusters were discovered. The majority of groundwater falls under cluster-1($n = 16$), which is divided into four subclusters. Cluster 2 had a total of six groundwater samples, which were further separated into two subclusters. Cluster 3 is almost entirely composed of deep groundwater, with the exception of BH-5. As demonstrated in Table 3, the second cluster consists of samples with lower average EC, K+, Na+, Ca2+, Mg 2+, and HCO3- values than the second and third clusters. Cluster-1 has a considerable variation in EC, K^+, Ca^{2+}, Mg^{2+}, and HCO_3^- between clusters 2 and 3. This third cluster consisted of groundwater with the greatest amounts of EC, TDS, K^+, Ca^{2+}, Mg^{2+}, and HCO_3^-, indicating a substantial water-rock interaction. Compared to the other two clusters, Cluster 3 (deep wells) had the lowest concentrations of SO_4^{2-}, PO_4^-, Cl^-, and NO_3^-, showing that shallow wells and springs depend on human activity.

Three significant clusters can be detected in the research region using the R-mode clustering. The first cluster consisted of EC, TDS, Na^+, HCO_3^-, Mg^{2+}, Ca^{2+}, and K^+, and interactions between rock and water predominated. The second cluster consists of florid, which has geological and human-made origins. The final cluster is mostly associated with the anthropogenic consequences of SO_4^{2-}, PO_4^-, NO_3^-, and Cl^-.

3.6.3. Principal Component Analysis (PCA). Principal component analysis simplifies several variables to a small number of components. Consequently, two main components explained 80.36 percent of the total variation of the study area (Table 4). Factor 1 had strong loadings on Na^+, K^+, Mg^{2+}, Ca^{2+}, HCO_3^-, EC, and TDS. The association of these parameters reflected the occurrence of dissolved solutes in water and can thus be characterized by the geogenic source (water-rock interaction) factor. Factor 2 had strong loading on PO_4^{2-}, SO_4^{2-}, Cl^-, and NO_3^- were mainly derived from anthropogenic activities, and it can thus be characterized as a human-induced interaction factor [52].

3.7. Water Quality Evaluation

3.7.1. Drinking Water Quality Evaluation. Generally, it is described as the effect of various water quality parameters on the total water quality [60]. It is a mathematical equation that combines several water-quality data points into a single number. Using a data visualization tool, researchers and policymakers may effectively communicate information concerning water quality [41, 61, 62]. Fifteen parameters (pH, EC, TDS, Ca^{2+}, Mg^{2+}, Na^+, K^+, Fe^{2+}, HCO_3^-, Cl^-, SO_4^{2-}, NO_3^-, F^-, TH, and PO_4^{2-}) have been used for the calculation (Table 5). Finally, the computed WQI values are classified into five categories (Table 6).

Based on the descriptive statistical analysis of WQI values for the study area, about 53.85% of the samples ($n = 14$) had "excellent" water quality. Approximately 26.9% of the samples ($n = 7$) fall into the "good" water class. Thirdly, the "poor" water class ($n = 2$) covered approximately 7.7% of the total sample. 11.55% of the sample was composed of the "very poor" water class ($n = 3$). It should be noted that all deep boreholes fall under poor water conditions (BH-3 and BH-5) or very poor water conditions (BH-1, BH-2, and BH-4). It is evident from these samples that the water samples are highly ionized and evolved at greater depths in the borehole. The spatial distribution of the water quality index in the present study area is shown in Figure 22.

3.7.2. Irrigation Water Quality Evaluation. Exercising irrigation action is essential in elevating the irrigation production rate and meeting the growing population's continuously increasing food demands [63]. Determining the suitability and vulnerability of groundwater quality for irrigation use is a crucial alarm and first aid for managing groundwater resources to diminish the impacts on irrigation [64]. Irrigation with poor-quality waters may bring undesirable elements to the soil in excessive quantities affecting its fertility [65]. The following multicriteria investigation approach was considered to be appropriate for evaluating the appropriateness of groundwater for irrigation purposes in the study area. The salinity risk was assessed by EC and TDS, the sodicity risk by SAR and Na%, the bicarbonate risk by RSC, and the permeability risk by MH and PI. Table 7 displays the computed values for Na%, SAR, MH, PI, RSC, EC, and TDS for irrigation water quality.

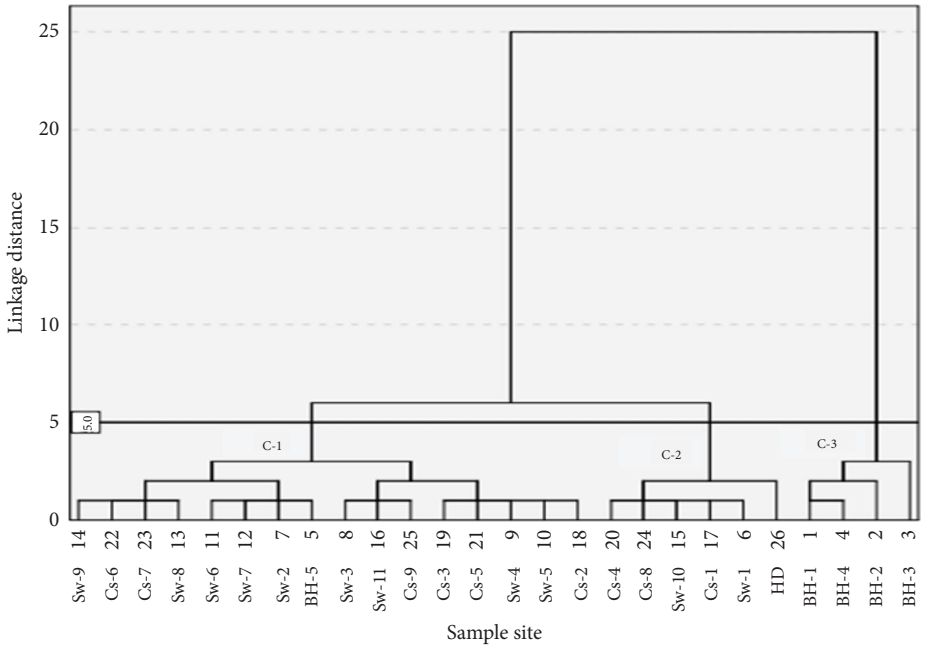

Figure 20: Hierarchical dendrogram clusters (Q-mode clustering).

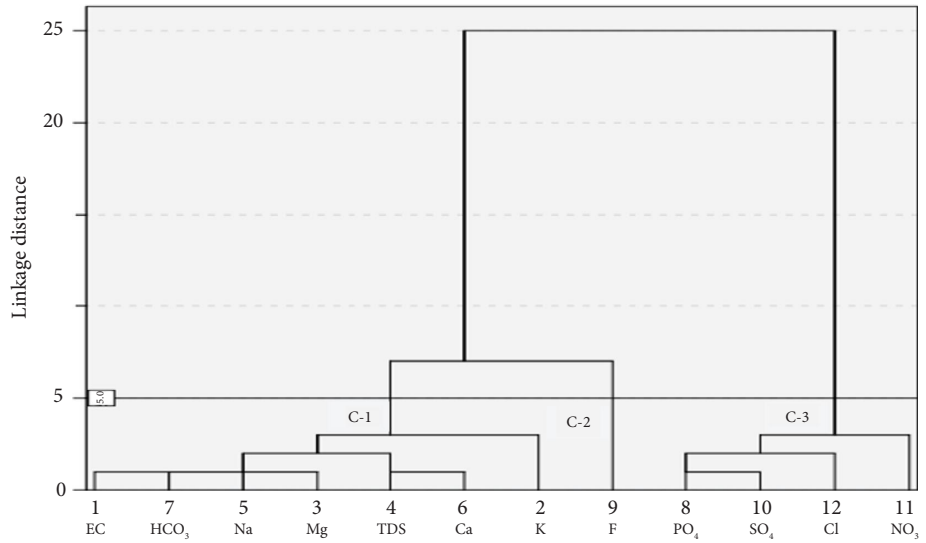

Figure 21: Hierarchical dendrogram cluster (R-mode clustering).

(1) Hazard based on EC and TDS. The salinity index is the most impactful water quality criterion on crop yield, according to [32]. As EC concentration rises, a plant's water intake decreases, which has a negative effect on its productivity. The higher the EC, despite the soil's apparent moisture, the less water is available to plants. As EC rises, the amount of plant-usable water in the soil solution decreases dramatically [66]. Total dissolved solids also affect the quality of irrigation water. The salinity hazard occurs when an accumulation of total dissolved salt in the plant root zone reduces crop yield [67].

From Table 8, samples are excellent, and seventeen samples are good, indicating no hazard based on TDS will arise by using the groundwater of the study area for irrigation. The remaining only one sample was doubtful, and the other three were unsuitable for irrigation due to the relatively higher values of TDS. This table also clearly shows that the tested samples for EC lay within a range of low hazard to very high hazard for irrigation use. Thus, four samples were low hazardous, seventeen samples were a medium hazard, 1 sample was high hazardous, and the remaining four samples were found to be a very high hazard for irrigation purposes.

Table 3: Mean concentrations of clustered parameters.

Parameter	Cluster-1, $n = 16$ Cs-2, Cs-3, Cs-5, Cs-6, Cs-7, Cs-9, Sw-2, Sw-3, Sw-4, Sw-5, Sw-6, Sw-7, Sw-8, Sw-9, Sw-11, and BH-5	Cluster-2, $n = 6$ HD,Cs-1,Cs-4,Cs-8,Sw-1,Sw-10	Cluster-3, $n = 4$ BH-1,BH-2,BH-3,BH-4
EC (μs/cm)	399.23	321.6	3847.5
TDS (mg/l)	230.518	287	2483.5
Ca^{2+} (mg/l)	13.148	7.23	2483.5
K^{+} (mg/l)	2.64	2.73	35.815
Na^{+} (mg/l)	47.53	29.6	138.85
Mg^{2+} (mg/l)	21.94	9.75	141.85
F^{2+} (mg/l)	0.19	0.24	0.455
Cl^{-} (mg/l)	20	8.1	2.59
SO_4^{2-} (mg/l)	8	4.5	2.1
PO_4^{2-} (mg/l)	1.02	1.26	0.88
HCO_3^{-} (mg/l)	249.41	163.58	1574.3
NO_3^{-} (mg/l)	9.07	8.34	0.663

n stands for the number of samples

Table 4: Factor loadings and eigenvalues matrix of each hydrogeochemical parameters.

Variable (mg/l) except EC (μs/cm)	Factor loading	
	Factor 1	Factor 2
TDS	**0.944**	0.077
EC	**0.956**	−0.044
Na^{+}	**0.883**	0.077
K^{+}	**0.798**	−0.276
Ca^{2+}	**0.944**	0.071
Mg^{2+}	**0.873**	0.190
HCO_3^{-}	**0.980**	0.064
NO_3^{-}	−0.882	**0.92**
SO_4^{-}	0.251	**0.873**
PO_4^{-}	0.051	**0.64**
Cl^{-}	0.107	**0.963**
F^{-}	0.41	0.387
Total eigenvalue	6.89	1.15
Explained variance%	68.914	11.447
Cumulative % of variance	68.912	80.319

Bold values show the strong correlations between the chemical components.

Table 5: World health organization (WHO) standards, weight (wi), and relative weight (Wi) for each parameter of the groundwater samples in the area.

Physicochemical parameter (mg/l) except pH (unitless) & EC (μS/cm)	WHO standard	Assigned weight (wi)	Relative weight (Wi)
pH	6.5–8.5	4	0.077
EC	1000	4	0.077
TDS	500	5	0.096
Ca^{2+}	75	3	0.058
Mg^{2+}	50	3	0.058
Na^{+}	200	3	0.058
K^{+}	12	3	00.058
HCO_3^{-}	120	3	0.058
Fe^{2+}	0.3	3	0.058
Cl^{-}	250	3	0.058
SO_4^{-}	250	3	0.058
NO_3^{-}	50	5	0.096
F^{-}	1.5	5	0.096
TH	300	3	0.058
PO_4^{2-}	10	2	0.038
		$\sum wi = 52$	$\sum Wi = 1$

Table 6: Classification and categorization of computed WQI values for human consumption [41].

WQI ranges	Type of water
≤50	Excellent ($n = 14$, 53.85%)
(50–100)	Good ($n = 7$, 26.9%)
[100–200)	Poor($n = 2$,7.7%)
[200–300)	Very poor ($n = 3$,11.55%)
≥300	Unfit for drinking (nil)

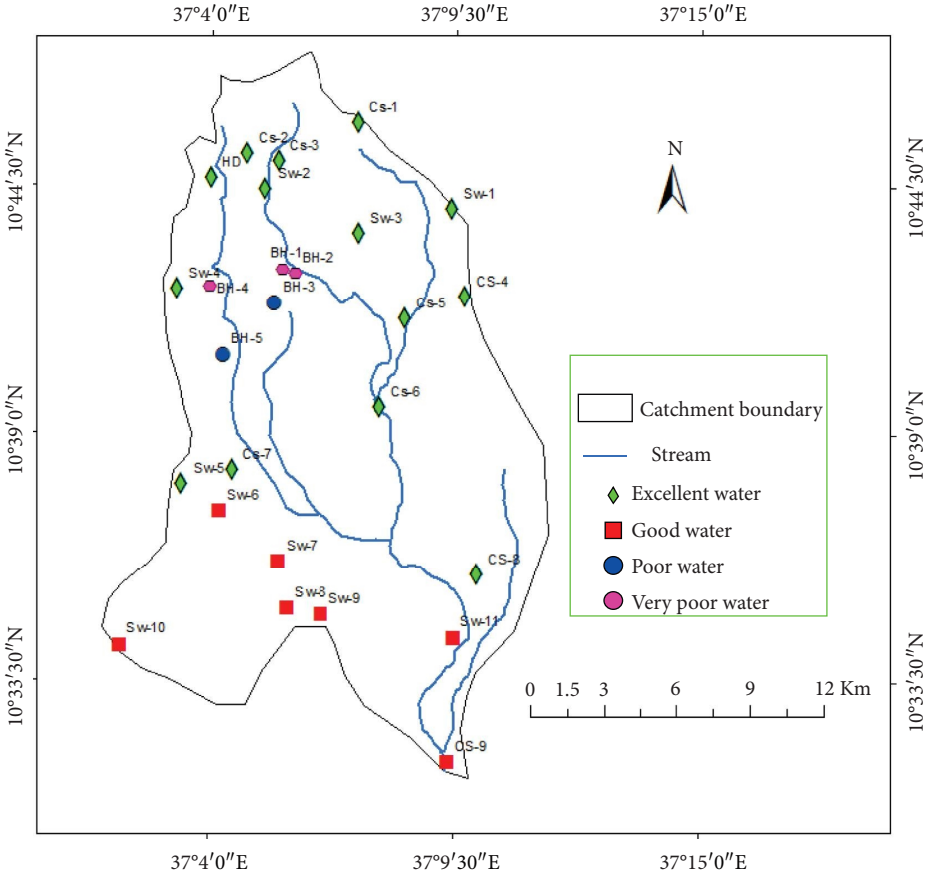

Figure 22: Spatial variability map of WQI.

Based on the salinity classification standard of the Wilcox plot, the hydrochemical samples ranged from low to very high salinity [69].

(2) Sodium Hazard Based on SAR and Na%. When excessive salt is present in irrigation groundwater, it can induce sodium hazard and reduce irrigation productivity by limiting the amount of water available for plant growth. Excess sodium in irrigation water can immobilize other nutrients, notably magnesium, calcium, and potassium, resulting in nutrient shortages in plants [70]. Because it assesses alkali/sodium risk, sodium adsorption ratio (SAR) is an important indicator for establishing the appropriateness of groundwater for irrigation. SAR and Na% were calculated using the following equations (9) and (10) [32]:

$$\text{Sodium percentage (NA\%)} = \frac{(\text{Na}^+ + \text{K}^+) \times 100}{\text{Ca}^{2+}\text{Mg}^{2+} + \text{Na}^+ + \text{K}^+} \cdots\cdots\cdots, \tag{9}$$

$$\text{Sodium adsorption ratio (SAR)} = \frac{\text{Na}^+}{\sqrt{(\text{Ca}^{2+}) + (Mg^{2+})/2}} \cdots\cdots\cdots. \tag{10}$$

Table 7: Computed values of Na%, SAR, MH, PI, RSC, EC, and TDS for irrigation water quality.

Well type	Na%	SAR	MH	PI	RSC	EC	TDS
BH-1	23.65	1.81	64.78	72.15	6.21	3360	2184
BH-2	20.21	1.6	90.37	92.22	9.98	5430	3555.5
BH-3	6.99	0.27	12	16.48	4.09	2260	1460
BH-4	28.78	1.49	57.85	66.84	8.8	4340	2734.5
BH-5	33.33	1.2	19.71	45.78	0.67	790	434.29
Sw-1	27.09	0.23	38.72	44.62	−0.21	179	300
Sw-2	25.67	0.38	42.71	49.55	0.19	398	189.4
Sw-3	14.39	0.32	23.93	32.06	0.01	345	334
Sw-4	10.63	0.26	39.87	45.64	0.37	352	351
Sw-5	11.46	0.24	38.11	43.09	0.3	425	324
Sw-6	11.61	0.44	61.37	65.58	−1.47	473	225
Sw-7	10.09	0.33	65.55	68.75	−0.49	420	201.1
Sw-8	9.02	0.34	55.56	59.28	−1.25	461	222
Sw-9	8.01	0.26	51.49	55.09	−0.8	398	189.5
Sw-10	14.73	0.24	45.03	51.16	0.39	422	267
Sw-11	16.18	0.36	29.24	37.95	0.81	620	358
Cs-1	18.15	0.36	25.62	37.08	0.36	240	226
Cs-2	19.61	0.43	25.37	38.55	0.16	298	142.7
Cs-3	13.08	0.33	20.43	30.19	0.01	102.2	95.8
CS-4	12.77	0.26	43.41	50	0.44	259	267
Cs-5	12.33	0.13	51.03	54.21	−1.72	164.4	78.1
Cs-6	12.1	0.34	41.52	48.15	0.11	392	186.9
Cs-7	21.13	0.38	46.84	52.71	0.42	351	167
CS-8	13.62	0.36	43.96	51.17	0.46	336	465
CS-9	10.54	0.34	42.47	47.9	−0.44	461	449
HD	2.95	0.07	68.09	68.93	−2.04	52.6	139

where all concentrations are expressed by meq/l.

All 26 samples evaluated in the research region had excellent SAR values, below 10, according to the criteria and values in Table 8, which implies no sodium toxicity will emerge from using groundwater from these groundwater for irrigation based on SAR. As indicated in Table 8, 19 of 26 examined groundwater samples show excellent sodium levels (Na%). Based on Na%, the remaining seven samples are good, showing that irrigation with groundwater from the study area will not increase sodium toxicity.

(3) Hazard Based on Residual Sodium Crbonate and Magnesium Hazard. Because of the high concentration of bicarbonates in irrigation groundwater, calcium and magnesium tend to precipitate. Residual sodium carbonate (RSC) was utilized to determine the danger of bicarbonate. Magnesium in groundwater makes soil alkaline. Hence, assessing magnesium hazard (MH) for irrigation is also helpful. By using equations (11) and (12), RSC and MH were calculated as follows [32]:

$$\text{Residual sodium carbonate}\,(RSC) = \left(CO_3^{2-} + HCO_3^{-}\right) - \left(Ca^{2+} + Mg^{2+}\right)\cdots \tag{11}$$

$$\text{Magnesium hazard (MH)} = \text{Magnesium hazard}\,(\text{MH}) = \frac{\text{Mg}^{2+} \times 100}{\text{Ca}^{2+} + \text{Mg}^{2+}}, \tag{12}$$

where all concentrations expressed by meq/l.

Twenty-two samples are within the suitable category of all the tested groundwater samples for RSC in the Yisr river catchment. The remaining four samples were found within the unsuitable range i.e., RSC > 2.5. According to [65], continuous use of water having an RSC of more than 2.5 meq/l leads to salt build-up, which may hinder the air and water movement by clogging the soil pores and lead to degradation of the physical condition of the soil. On the other hand, based on magnesium hazard, 16 samples lay within the suitable group, and the remaining ten samples were found in the range of the unsuitable class. In these samples, the high magnesium in irrigation water impacts soil quality by converting it to alkali, which eventually reduces its productivity..

(4) Permeability Index (PI). The soil permeability is affected by the continuous usage of irrigation water as it is affected by the soil's Ca2+, Mg2+, Na+, and HCO_3^- concentrations. Assessing the suitability of study area groundwater for irrigation purposes based on the permeability index (PI) is given by equation (equation (13), (41)) where concentrations are expressed in meq/l.

Table 8: Classification of groundwater for irrigation based on Na%, SAR, MH, PI, RSC, EC, and TDS [68].

Parameter	Range	Water type/classification	Number of samples
SAR	<10	Excellent (S1)	All 26 samples
	10–18	Good (S2)	—
	18–26	Doubtful (S3)	—
	>26	Unsuitable (S4)	—
EC (μS/cm)	<250	Low	HD,Cs-5, Cs-3, and Sw-1
	250–750	Medium	All the rest 17 samples
	750–2250	High	BH-5
	>2250	Very high	BH-1, BH-2, BH-3, and BH-4
RSC	<1.25	Good	All the rest 22 samples
	1.25–2.5	Doubtful	—
	>2.5	Unsuitable	BH-1, BH-2, BH-3, and BH-4
Na% (Adimalla, 2018)	<20	Excellent	All the rest 19 samples
	20–40	Good	BH-1, BH-2, BH-4, BH,5, SW-1,SW-2, and Cs-7
	40–60	Permissible	—
	60–80	Doubtful	—
	>80	Unsuitable	—
MH	<50	Suitable	All the rest 16 samples
	>50	Unsuitable	BH-1, BH, 2, BH-4,Sw-6, Sw-7,Sw-8, Sw-9, Cs-5, and HD
PI	Class-I &II	75% permissible	All the rest 25 samples
	Class -III	25% permissible	BH-3
TDS (mg/l)	<175	Excellent	Cs-2, Cs-3, Cs-5, Cs-7, and HD
	175–525	Good	All the rest 17 samples
	525–1400	Permissible	—
	1400–2100	Doubtful	BH-3
	>2100	Unsuitable	BH-1, BH-2, and BH-4

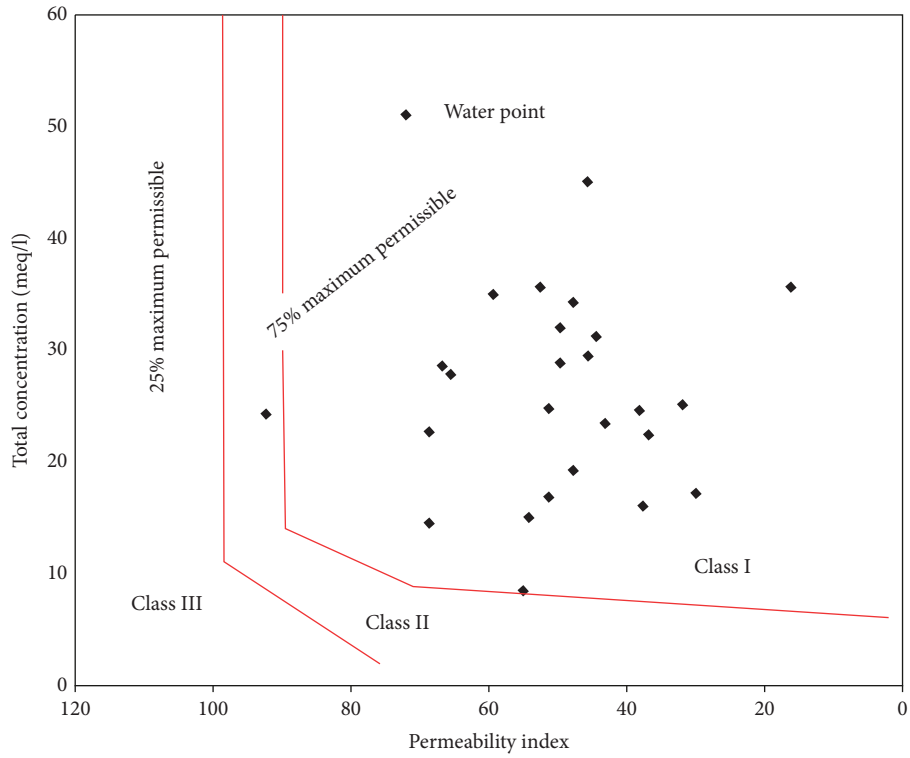

Figure 23: Wilcox diagram represents the quality of the Yisr catchment groundwater based on the permeability index.

$$\mathrm{PI} = \frac{\mathrm{Na}^{+} + \sqrt{\mathrm{HCO}_3^{-}}}{\mathrm{Ca}^{2+} + \mathrm{Mg}^{2+} + \mathrm{Na}^{+}} \times 100. \quad (13)$$

Using the permeability index diagram, it is feasible to describe the significance and meaning of quality assessment as follows: class I and II waters are suitable for irrigation if their maximum permeability is at least 75%, whereas class III waters are unsuitable for irrigation if their maximum permeability is less than 25% [68] According to Figure 23, out of 26 examined groundwater samples, 96.2% and 3.8%, respectively, fell into classifications I and II, which are appropriate for irrigation in nearly all soil types. The studied groundwater samples did not fall into the undesirable (Class III) category for irrigation.

4. Conclusions

Groundwater is the main source of water for drinking, farming, and industry (Bure Integrated AgroIndustry Park) in catchment areas. However, there has been no systematic study of the hydrogeochemical properties of groundwater in the study area. The main objective of this study was to investigate the hydrogeochemical characteristics and suitability of water for irrigation and drinking. An individual ionic signature, interionic ratio plot, graphical plot, water quality index (WQI) for drinking, agricultural indices, and multivariate statistical analysis (PCA and HCA) were used. Totally, 26 groundwater samples from shallow wells (<60 m), including springs and deep wells (>60 m), along with 17 parameters such as pH, temperature, EC, TDS, TH, K^+, Na^+, Ca^{2+}, Mg^{2+}, Fe^{2+}, Cl^-, HCO_3^-, CO_3^-, SO_4^{2-}, F^-, PO_4^{2-}, and NO_3^-, were used. The box plot diagram showed the major dominant ions in descending order of $Ca^{2+} > Mg^{2+} > Na^+ > K^+$ and $HCO_3^{2-} > Cl^- > SO_4^{2-} > NO_3^- > F^-$ a trend for cations and anions, respectively. From the piper triangular plot diagram, the study area's groundwater samples were found exclusively Ca-HCO_3 groundwater type.

The chloroalkaline indices suggested that the dominant processes in the catchment were forward ion exchange and reverse ion exchange. The chemical composition of shallow wells and springs portrayed freshwater, suggesting limited water-rock interaction, shallow groundwater circulation, shallow flow, and a low residence time. Deep groundwater wells are brackish, indicating that these waters have undergone extensive water-rock interaction, stayed for a long time and had deep or regional flow. Two R-factor loadings (PCA analysis) were used to explain the existence of anthropogenic and geogenic sources. Three clusters were identified from the Q-mode dendrogram. The 3rd cluster had the most significant linkage distance among all the clusters, indicating that the groundwater sample in this cluster was geochemically distinct from the other two clusters. This cluster consisted of deep wells. Based on the R-mode dendrogram, SO42-, PO42-, NO3-, and Cl- forming their clusters indicates that the source of these ions is human-induced activity, also known as anthropogenic sources.

WQI showed water qualities ranged from excellent to very poor water where the majorities, 53.85%, are excellent, followed by 26.9%, are good. The calculated indices for agricultural water quality indicated that water quality in

most collected samples is in a good and excellent category; however, EC, RSC, MH, and TDS indices in deep groundwater wells have been found hazardous. The research has believed to give insight into characteristics of hydrogeochemistry and groundwater quality for irrigation and drinking purpose of the area, which is very important in water resource management and development methods by giving directions for groundwater management options.

Data Availability

All data that support the findings of this study are included in the manuscript.

Conflicts of Interest

The authors declare that they have no conflicts of interest.

References

[1] S. V. Mukate, D. B. Panaskar, V. M. Wagh, and S. J. Baker, "Understanding the influence of industrial and agricultural land uses on groundwater quality in semiarid region of Solapur, India," *Environment, Development and Sustainability*, vol. 22, pp. 3207–3238, 2020.

[2] D. Marghade, D. B. Malpe, and N. Subba Rao, "Applications of geochemical and multivariate statistical approaches for the evaluation of groundwater quality and human health risks in a semi-arid region of eastern Maharashtra, India," *Environmental Geochemistry and Health*, vol. 43, no. 2, pp. 683–703, 2021.

[3] A. Kadam, V. Wagh, S. Patil, B. Umrikar, R. Sankhua, and J. Jacobs, "Seasonal variation in groundwater quality and beneficial use for drinking, irrigation, and industrial purposes from Deccan Basaltic Region, Western India," *Environmental Science and Pollution Research*, vol. 28, no. 20, pp. 26082–26104, 2021.

[4] N. Subba Rao, "Spatial distribution of quality of groundwater and probabilistic non-carcinogenic risk from a rural dry climatic region of South India," *Environmental Geochemistry and Health*, vol. 43, no. 2, pp. 971–993, 2021.

[5] World bank, *Drinking-water Quality in Ethiopia*, Central statistical agency of Ethiopia, Addis Ababa, Ethiopia, 2017.

[6] J. Fito, G. Bultosa, and H. Kloos, "Correction to: physicochemical and heavy metal constituents of the groundwater quality in haramaya woreda, oromia regional state, Ethiopia," *International Journal of Energy and Water Resources*, vol. 3, no. 2, p. 167, 2019.

[7] E. B. Chebet, J. K. Kibet, and D. Mbui, "The assessment of water quality in river Molo water basin, Kenya," *Applied Water Science*, vol. 10, no. 4, p. 92, 2020.

[8] R. A. Freeze and J. A. Cherry, *Groundwater*, Prentice-Hall, Englewood Cliffs, NJ, USA, 1978.

[9] K. R. Karanth, *Ground Water Assessment: Development and Management*, Tata McGraw-Hill Publishing Company Limited, New Delhi, 1987.

[10] M. N. Sara and R. Gibbons, "Organization and analysis of water quality data," in *Practical Handbook of Groundwater Monitoring*, D. M. Nielsen, Ed., Lewis Publishers, Michigan, 1991.

[11] C. Güler, G. D. Thyne, J. E. McCray, and K. A. Turner, "Evaluation of graphical and multivariate statistical methods for classification of water chemistry data," *Hydrogeology Journal*, vol. 10, no. 4, pp. 455–474, 2002.

[12] D. Machiwal and M. K. Jha, "Identifying sources of groundwater contamination in a hard-rock aquifer system using multivariate statistical analyses and GIS-based geostatistical modeling techniques," *Journal of Hydrology: Regional Studies*, vol. 4, pp. 80–110, 2015.

[13] M. F. Howladar, M. A. Al Numanbakth, and M. O. Faruque, "An application of water quality index (WQI) and multivariate statistics to evaluate the water quality around maddhapara granite mining industrial area, dinajpur, Bangladesh," *Environmental Systems Research*, vol. 6, no. 1, p. 13, 2018.

[14] V. Cloutier, R. Lefebvre, R. Therrien, and M. M. Savard, "Multivariate statistical analysis of geochemical data as indicative of the hydrogeochemical evolution of groundwater in a sedimentary rock aquifer system," *Journal of Hydrology*, vol. 353, no. 3-4, pp. 294–313, 2008.

[15] C. Steube, S. Richter, and C. Griebler, "First attempts towards an integrative concept for the ecological assessment of groundwater ecosystems," *Hydrogeology Journal*, vol. 17, no. 1, pp. 23–35, 2009.

[16] V. M. Wagh, S. V. Mukate, D. B. Panaskar, A. A. Muley, and U. L. Sahu, "Study of groundwater hydrochemistry and drinking suitability through Water Quality Index (WQI) modelling in Kadava river basin. India," *SN Applied Sciences*, vol. 1, no. 10, p. 1251, 2019.

[17] B. Qu, Y. L. Zhang, S. C. Kang, and M. Sillanpää, "Water quality in the Tibetan plateau: major ions and trace elements in rivers of the "water tower of asia," *Science of the Total Environment*, vol. 649, pp. 571–581, 2019.

[18] A. Gidey, "Geospatial distribution modeling and determining suitability of groundwater quality for irrigation purpose using geospatial methods and water quality index (WQI) in Northern Ethiopia," *Applied Water Science*, vol. 8, no. 3, p. 82, 2018.

[19] G. T. Bawoke and Z. L. Anteneh, "Spatial assessment and appraisal of groundwater suitability for drinking consumption in Andasa watershed using water quality index (WQI) and GIS techniques: Blue Nile Basin, northwestern Ethiopia," *Cogent Engineering*, vol. 7, no. 1, Article ID 1748950, 2020.

[20] M. K. Jha, A. Chowdhury, V. M. Chowdary, and S. Peiffer, "Groundwater management and development by integrated remote sensing and geographic information systems: prospects and constraints," *Water Resources Management*, vol. 21, no. 2, pp. 427–467, 2007.

[21] G. S. Solangi, A. A. Siyal, M. M. Babar, and P. Siyal, "Application of water quality index, synthetic pollution index, and geospatial tools for the assessment of drinking water quality in the Indus Delta, Pakistan," *Environmental Monitoring and Assessment*, vol. 191, no. 12, p. 731, 2019.

[22] C. A. Reyes-Toscano, R. Alfaro-Cuevas-Villanueva, R. Cortés-Martínez et al., "Hydrogeochemical characteristics and assessment of drinking water quality in the Urban Area of Zamora, Mexico," *Water*, vol. 12, no. 2, p. 556, 2020.

[23] J. T. Liu, Z. J. Gao, M. Wang et al., "Hydrochemical characteristics and possible controls in the groundwater of the yarlung zangbo river valley, China," *Environmental Earth Sciences*, vol. 78, no. 3, p. 76, 2019.

[24] L. Pei-Yue, Q. Hui, W. Jian-Hua, and J. Wu, "Groundwater quality assessment based on improved water quality index in Pengyang County, Ningxia. Northwest China," *E-Journal of Chemistry*, vol. 7, no. s1, pp. 209–216, 2010.

[25] M. V. Prasanna, S. Chidambaram, T. V. Gireesh, T. V. Jabir Ali, and J. Ali, "A study on hydrochemical characteristics of surface and sub-surface water in and around Perumal Lake, Cuddalore District, Tamil Nadu South India," *Environmental Earth Sciences*, vol. 63, no. 1, pp. 31–47, 2011.

[26] A. Bouderbala, "Assessment of water quality index for the groundwater in the Upper Cheliff Plain, Algeria," *Journal of the Geological Society of India*, vol. 90, no. 3, pp. 347–356, 2017.

[27] V. Sunitha and B. M. Reddy, "Geochemical characterization, deciphering groundwater quality using pollution index of groundwater (PIG), water quality index (WQI) and geographical information system (GIS) in hard rock aquifer, South India," *Applied Water Science*, vol. 12, no. 3, p. 41, 2022.

[28] L. Tsige, "Geology of Bure map sheet," Geological Survey of Ethiopia, Addis Ababa, Ethiopia, (NC-37/5) memoir no 18, 2008.

[29] T. Ayenew, F. Wisotzky, M. Demlie, and S. Wohnlich, "Hierarchical cluster analysis of hydrochemical data as a tool for assessing the evolution and dynamics of groundwater across the Ethiopian rift," *International Journal of the Physical Sciences*, vol. 4, no. 2, pp. 076–090, 2009.

[30] Apha, *Standard Methods for the Examination of Water and Wastewater*, American Public Health Association/American Water Works Association/Water Environment Federation, Washington DC, 2005.

[31] M. R. Guggenmos, C. J. Daughney, B. M. Jackson, and U. Morgenstern, "Regional-scale identification of groundwater-surface water interaction using hydrochemistry and multivariate statistical methods, Wairarapa Valley, New Zealand," *Hydrology and Earth System Sciences*, vol. 15, no. 11, pp. 3383–3398, 2011.

[32] P. Ravikumar, R. Somashekar, and M. Angami, "Hydrochemistry and evaluation of groundwater suitability for irrigation and drinking purposes in the Markandeya River basin, Belgaum District, Karnataka State, India," *Environmental Monitoring and Assessment*, vol. 173, pp. 459–487, 2011.

[33] F. Jenn, C. Kofahl, M. Müller, J. Radschinski, and H. J. Voigt, "Interpretation of geological, hydrogeological, and geochemical results," in *Environmental Geology*,Springer, Berlin, Heidelberg, 2007.

[34] A. V. Udayanapillai and M. Kaliammal, "Groundwater characterization and quality assessment by using GIS and Geostatistics from Pandalgudi region, Virudhunagar district, Tamilnadu, India," *International journal of research in environmental science*, vol. 2, no. 4, pp. 1–16, 2016.

[35] K. A. Christian, D. K. Dodoo, and B. K. Kortasi, "The hydrochemistry of groundwater in some communities in the Ayensu River Basin in the central region of Ghana," *Journal of Environment and Earth Science*, vol. 4, no. 20, pp. 50–65, 2014.

[36] Q. Zheng, T. Ma, Y. Wang, Y. Yan, L. Liu, and L. Liu, "Hydrochemical characteristics and quality assessment of shallow groundwater in Xincai River Basin, northern China," *Procedia Earth and planetary science*, vol. 17, pp. 368–371, 2017.

[37] O. Ghesquière, J. Walter, R. Chesnaux, and A. Rouleau, "Scenarios of groundwater chemical evolution in a region of the Canadian shield based on multivariate statistical analysis," *Journal of Hydrology: Regional Studies*, vol. 4, pp. 246–266, 2015.

[38] N. Voutsis, E. Kelepertzis, E. Tziritis, and A. Kelepertsis, "Assessing the hydrogeochemistry of groundwaters in ophiolite areas of Euboea Island, Greece, using multivariate statistical methods," *Journal of Geochemical Exploration*, vol. 159, pp. 79–92, 2015.

[39] S. N. Sethy, T. H. Syed, A. Kumar, and D. Sinha, "Hydrogeochemical characterization and quality assessment of groundwater in parts of Southern Gangetic plain," *Environmental Earth Sciences*, vol. 75, no. 3, p. 232, 2016.

[40] A. J. Adewumi, A. Y. B. Anifowose, F. O. Olabode, and T. A. Laniyan, "Hydrogeochemical characterization and vulnerability assessment of shallow groundwater in basement complex area, southwest Nigeria," *Contemporary Trends in Geoscience*, vol. 7, no. 1, pp. 72–103, 2018.

[41] S. Singh and A. Hussian, "Water quality index development for groundwater quality assessment of greater Noida subbasin, Uttar Pradesh, India," *Cogent Engineering*, vol. 3, no. 1, Article ID 1177155, 2016.

[42] C. R. Ramakrishnaiah, C. Sadashivaiah, and G. Ranganna, "Assessment of water quality index for the groundwater in Tumkur Taluk, Karnataka State, India," *E-Journal of Chemistry*, vol. 6, no. 2, pp. 523–530, 2009.

[43] Who, *Guidelines for Drinking Water Quality*, World Health Organization, Switzerland, 4th edition, 2011.

[44] J. D. Hem, *Study and Interpretation of the Chemical Characteristics of Natural Water, United States Government Printing Office*, U.S Geological Survey, Reston, VA, USA, 1985.

[45] N. Kresic, *Groundwater Resources Sustainability, Management, and Restoration*, McGraw-Hill, New York, NY, USA, 2009.

[46] S. N. Davis and R. J. M. Dewiest, *Groundwater in Fractured Rocks*, Water Education Foundation, Sacramento, Calif, 1966.

[47] G. H. Jeelani, R. A. Shah, and A. Hussain, "Hydrogeochemical assessment of groundwater in kashmir valley, India," *Journal of Earth System Science*, vol. 123, no. 5, pp. 1031–1043, 2014.

[48] D. K. Todd and L. W. Mays, *Groundwater Hydrology*, Wiley, Hoboken, NJ, 2005.

[49] M. B. Tolera, H. Choi, S. W. Chang, and I. M. Chung, "Groundwater quality evaluation for different uses in the lower Ketar Watershed, Ethiopia," *Environmental Geochemistry and Health*, vol. 42, no. 10, pp. 3059–3078, 2020.

[50] L. Elango and R. Kannan, "Chapter 11 Rock–water interaction and its control on chemical composition of groundwater," *Concepts and Applications in Environmental Geochemistry*, vol. 5, pp. 229–243, 2007.

[51] R. J. Gibbs, "Mechanisms controlling world water chemistry," *Science*, vol. 170, no. 3962, pp. 1088–1090, 1970.

[52] J. Chen, Q. Huang, Y. Lin et al., "Hydrogeochemical characteristics and quality assessment of groundwater in an irrigated region, northwest China," *Water*, vol. 11, no. 1, pp. 96–18, 2019.

[53] T. Ayenew, M. GebreEgziabher, S. Kebede, and S. Mamo, "Integrated assessment of hydrogeology and water quality for groundwater-based irrigation development in the Raya valley northern Ethiopia," *Water International*, vol. 38, no. 4, pp. 480–492, 2013.

[54] N. Aghazadeh, M. Chitsazan, and Y. Golestan, "Hydrochemistry and quality assessment of groundwater in the Ardabil area, Iran," *Applied Water Science*, vol. 7, no. 7, pp. 3599–3616, 2017.

[55] S. Deepa and S. Venkateswaran, "Appraisal of groundwater quality in upper Manimuktha sub-basin, Vellar river, Tamil Nadu, India by using water quality index (WQI) and multivariate statistical techniques," *Modeling Earth Systems and Environment*, vol. 4, no. 3, pp. 1165–1180, 2018.

[56] L. Kaur, M. S. Rishi, S. Sharma, B. Sharma, R. Lata, and G. Singh, "Hydrogeochemical characterization of groundwater in alluvial plains of river Yamuna in northern India: an insight of controlling processes," *Journal of King Saud University Science*, vol. 31, no. 4, pp. 1245–1253, 2019.

[57] K. Srinivasamoorthy, S. Chidambaram, M. V. Prasanna, M. Vasanthavihar, J. Peter, and P. Anandhan, "Identification of major sources controlling groundwater chemistry from a hard rock terrain — a case study from Mettur taluk, Salem district, Tamil Nadu, India," *Journal of Earth System Science*, vol. 117, no. 1, pp. 49–58, 2008.

[58] H. Schoeller, "Qualitative evaluation of groundwater resources," *Methods and techniques of groundwater investigations and development*, pp. 54–83, 1965.

[59] C. N. Mgbenu and J. C. Egbueri, "The hydrogeochemical signatures, quality indices and health risk assessment of water resources in Umunya district, southeast Nigeria," *Applied Water Science*, vol. 9, no. 1, pp. 22–19, 2019.

[60] R. D. Harkins, "An objective water quality index," *Water pollution control federation*, vol. 46, no. 3, pp. 588–591, 1974, http://www.jstor.com/stable/25038160 E.

[61] T. T. Aragaw and G. Gnanachandrasamy, "Evaluation of groundwater quality for drinking and irrigation purposes using GIS-based water quality index in urban area of Abaya-Chemo sub-basin of Great Rift Valley, Ethiopia," *Applied Water Science*, vol. 11, no. 9, p. 148, 2021.

[62] B. A. Berhe, "Evaluation of groundwater and surface water quality suitability for drinking and agricultural purposes in Kombolcha town area, eastern Amhara region, Ethiopia," *Applied Water Science*, vol. 10, no. 6, p. 127, 2020.

[63] M. A. Molla and Y. D. Fitsume, "Irrigation water quality of river Kulfo and its implication in irrigated agriculture, southwest Ethiopia," *International Journal of Water Resources and Environmental Engineering*, vol. 9, no. 6, pp. 127–132, 2017.

[64] A. Gidey, "Geospatial distribution modeling and determining suitability of groundwater quality for irrigation purpose using geospatial methods and water quality index (WQI) in Northern Ethiopia," *Applied Water Science*, vol. 8, no. 3, pp. 82–16, 2018.

[65] T. Kaur, R. Bhardwaj, and S. Arora, "Assessment of groundwater quality for drinking and irrigation purposes using hydrochemical studies in Malwa region, southwestern part of Punjab, India," *Applied Water Science*, vol. 7, pp. 3301–3316, 2017.

[66] B. Kumar, U. K. Singh, and S. N. Ojha, "Evaluation of geochemical data of Yamuna River using WQI and multivariate statistical analyses: a case study," *International Journal of River Basin Management*, vol. 17, no. 2, pp. 143–155, 2019.

[67] M. Jain, L. Dadhich, and S. Kalpana, "Water quality assessment of kishan pura dam, baran, Rajasthan, India," *Nature Environment and Pollution Technology*, vol. 10, no. 3, pp. 405–408, 2011.

[68] N. Adimalla, "Groundwater quality for drinking and irrigation purposes and potential health risks assessment: a case study from semi-arid region of south India," *Exposure and Health*, vol. 11, no. 2, pp. 109–123, 2018.

[69] L. V. Wilcox, *Classification and Use of Irrigation Waters*, USDA, 1955.

[70] H. Soleimani, O. Nasri, B. Ojaghi et al., "Data on drinking water quality using water quality index (wqi) and assessment of groundwater quality for irrigation purposes in qorveh & dehgolan, Kurdistan, Iran," *Data in Brief*, vol. 20, pp. 375–386, 2018.